

Ultra-high surface area mesoporous carbons for colossal pre combustion CO₂ capture and storage as materials for hydrogen purification

Michael Cox, and Robert Mokaya*

School of Chemistry, University of Nottingham, University Park, NG7 2RD Nottingham, UK.

*r.mokaya@nottingham.ac.uk

Abstract

Carbon capture and storage (CCS) by solid adsorbents is currently attracting a great deal of attention. In this study, a new direction in the treatment of activateable carbon-containing precursors generated a family of mesoporous carbons that possess extremely high mesopore volume and hardly any microporosity. The mesoporous carbons, with up to 95% mesoporosity, have ultra-high surface area (2800 – 4000 m²g⁻¹) and pore volume (2.5 – 3.6 cm³g⁻¹). The porosity of the carbons, i.e., mesopores of size 25 - 50 Å and hardly any micropores, is favourable for CO₂ uptake under conditions that are relevant to pre combustion CCS, i.e., 25 °C and pressure of 20 to 50 bar. The best performing carbons have near total absence of micropores; our findings suggest that the presence of microporosity is a limiting factor in the CO₂ uptake capacity especially at high pressure (30 – 50 bar). The gravimetric (mmol g⁻¹) CO₂ uptake capacity of the mesoporous carbons is impressive; up to 28 (20 bar), 37 (30 bar), 46 (40 bar) and 55 (50 bar), which is equivalent to 2.42 g of CO₂ per g of carbon. Furthermore, due to their packing density (0.25 – 0.4 g cm⁻³), the mesoporous carbons exhibit colossal volumetric CO₂ uptake (in g l⁻¹) of up to 480 (20 bar), 640 (30 bar), 780 (40 bar) and 930 (50 bar). The performance of the mesoporous carbons is such that, at 30 bar, they can hold more than 10 times the CO₂ in a pressurized cylinder, and at 50 bar can store up to 470 cm³ cm⁻³. The all-round pre combustion CCS performance of the mesoporous carbons is significantly higher than that of the best carbons to date, and outperforms that of benchmark materials such as metal organic frameworks (MOFs). The carbons are highly suited, in terms of their CO₂ adsorption capacity and CO₂ selectivity over H₂, as materials for hydrogen purification under syngas flow conditions.

Introduction

There are two main ways by which the increase in levels of atmospheric carbon dioxide can be tackled, namely, (i) reducing the use of carbon-based fossil fuels by moving over to low carbon emission energy sources or simply reducing consumption, and (ii) removal of carbon dioxide from the atmosphere via capture and storage.¹⁻⁵ The latter requires materials that can efficiently capture and store CO₂;^{1,3,6} a significant proportion of the CO₂ in the atmosphere comes from burning (combustion) of fossil fuels for energy production.³ A wide range of materials have been studied for application in carbon capture and storage (CCS) via physical adsorption and/or separation.^{3,6-10} The materials studied so far, and which have performed admirably, are dominated by porous carbons,¹¹⁻¹⁴ zeolites¹⁵⁻¹⁷ and metal organic frameworks (MOFs).^{18,19} Due to their structural flexibility and stability (chemical and mechanical), light-weight porous carbons have emerged as promising adsorbents for CCS.¹¹⁻¹⁴ Recent studies have shown that the control and optimisation of pore size and surface area of porous carbons can provide a very useful tool in generating materials tailored towards CO₂ capture under either pre or post combustion (of fossil fuels) conditions.²⁰⁻²⁶

It has been demonstrated by several studies that to maximise CO₂ uptake at low pressure (i.e., post combustion conditions) porous carbons need to have a high surface area arising from small micropores of size 7 – 9 Å.^{8-14,27-35} On the other hand, the presence of small micropores can limit the level of pore volume achieved, which is inimical to material requirements for pre combustion CO₂ capture, which normally occurs at high (> 20 bar) pressure.³⁶ With regard to high pressure CCS, which is akin to conditions for pre combustion CO₂ storage, we have recently shown that carbons that possess both micropores and mesopores have improved storage of CO₂ at high pressure; up to 29.5, 34.5 and 38.3 mmol g⁻¹ at 25 °C and 30, 40 and 50 bar, respectively.³⁷ Furthermore, such micro-mesoporous materials show enhanced CO₂ working capacity storage for pressure swing application (PSA) systems arising from a combination of

greater CO₂ capture at high pressure and diminished uptake at the lower regeneration pressures.³⁷ Other researchers have also, recently, reported what are claimed to be record levels of high pressure CO₂ storage in micro-mesoporous carbons derived from (i) polyaniline cross-linked polymer networks (storage capacity of 28.3, 32.5 and 34.9 mmol g⁻¹ at 25 °C and 30, 40 and 50 bar, respectively),³⁸ or (ii) asphalt (storage capacity of 35.2 mmol g⁻¹ at 25 °C and 50 bar).³⁹ A common feature of the previously explored materials, which currently constitute the benchmark for high pressure CO₂ storage in porous carbons, is that they have very high surface area (3400 – 4200 m²g⁻¹).³⁷⁻³⁹ However, they also contain a significant amount of microporosity, which is not beneficial for high pressure (i.e., pre combustion) CO₂ storage; we have shown that the introduction of mesoporosity, along with a decrease in the proportion of microporosity, improves high pressure CO₂ storage.³⁷

It would appear, therefore, that the optimum porosity for pre combustion high pressure CO₂ uptake in carbons may tend towards high surface area materials that are devoid of microporosity or have minimal levels of microporosity. Such a class of materials does not currently exist. To test our hypothesis on the role of mesoporosity *visa-vis* microporosity, we have explored new routes for the preparation of porous carbons that go beyond currently accepted limits in an effort to generate materials with very low levels of microporosity and have assessed their high pressure CO₂ uptake under conditions similar to those used for pre combustion CCS involving, for example, the purification of syngas in power stations. Syngas, typically derived from hydrocarbons and coals, mainly contains 71–75% H₂, 15–20% CO₂, and ca. 5% of other gases (CH₄, CO, H₂O). The syngas is used as fuel in integrated gasification and combined cycle (IGCC) systems that incorporate steps for the pre combustion removal and sequestration of CO₂ in order to enrich the H₂ content.^{40,41} Removal of CO₂ improves the burning properties and also reduces the amount of CO₂ released by combustion of the syngas.^{40,41} Purification of the syngas, i.e. removal of CO₂, may be achieved via solvent

washing systems although solid adsorbents may also be used.⁴⁰⁻⁴⁴ A key requirement of any adsorbent for syngas (or H₂) purification is a high CO₂ adsorption capacity and selectivity for CO₂ over H₂, and thus there is need to develop solid state absorbers with improved CO₂ capacity and selectivity under pre combustion CCS conditions.

This study unravels interesting trends between the high pressure CO₂ uptake and the proportion of mesoporosity and/or microporosity in high surface area carbons and illustrates how the porosity may be tailored toward exceptional and hitherto unreached levels of moderate to high pressure CO₂ adsorption (both in terms of gravimetric and volumetric capacity), that are relevant to pre combustion CCS and hydrogen purification in general.

Experimental Section

Materials synthesis

The starting materials (precursors) used were polypyrrole and eucalyptus wood sawdust. The wood sawdust (designated as SD) was used after conversion to hydrochar,^{20,21} while the polypyrrole (designated as PPy), was prepared by adding 3 g of pyrrole to 200 mL of 0.5 M FeCl₃ aqueous solution and magnetically stirring at room temperature for 2 h, following which the resulting solid product (PPy) was separated by filtration, washed with distilled water and dried in an oven at 120 °C. The PPy or SD were activated by mixing with KOH, in an agate mortar, at predetermined KOH/PPy or KOH/SD hydrochar ratios followed by heating at 700 to 900 °C. The KOH/Precursor ratios used (3, 4 or 5) were those that were expected to offer high levels of activation. In a typical activation process the KOH/Precursor mixture was heated under a flow of nitrogen in a tube furnace to the desired temperature (700, 800 or 900 °C) at a ramp rate of 3 °C min⁻¹ and then held at the target temperature for 1 h. The resulting carbonaceous material was washed with 10 wt% HCl to remove any inorganic salts, and then washed several times with water (until the water was at pH 7), followed by drying in an oven at 120 °C. The

carbons from PPy or SD were designated as PPY-xT or SD-xT, respectively, where x is the KOH/Precursor ratio and T is the activation temperature. We also prepared samples of compactivated carbon^{20,21,45} via a modified route that included compaction of the KOH/Precursor mixture prior to thermal treatment. The KOH/PPy or KOH/SD hydrochar mixture, at a ratio of 4, was compacted for 10 min at a load of 10 tonnes in a 1.3 cm diameter die, equivalent to compaction pressure of 740 MPa. The resulting disk/pellet was placed in an alumina boat and heated in a horizontal furnace to 800 °C at heating ramp rate of 3 °C min⁻¹ under a nitrogen gas flow and held at 800 °C for 1 h. The resulting compactivated carbon was washed and dried as described above except that no stirring was used during the washing steps. The compactivated carbons were designated as MPPY-4800 (from PPy) and MSD-4800 (from SD).

We also prepared, for comparison purposes, a highly microporous carbon as follows; Hydrochar was obtained by heating, at a ramp rate of 5 °C min⁻¹, 6.4 g of cellulose acetate (CA) in 20 mL of water in a stainless steel autoclave to 250 °C for 2 h. The resulting hydrochar was obtained by filtration and dried overnight in an oven at 112 °C, and then activated as described above at KOH/CA hydrochar ratio of 4 and 700 °C. The resulting activated carbon (denoted as CA-4700) was washed as described above and dried at 112 °C.

Materials Characterisation

Powder X-ray diffraction (XRD) patterns were recorded using a PANalytical X'Pert PRO diffractometer with Cu- K_{α} radiation, operating at 40 kV and 40 mA with 0.02° step size and 30 s step time. Elemental (C, H, N and O) analysis was performed using a model CE-440 Elemental Analyzer (Exeter Analytical). Thermogravimetric analysis (TGA) was performed using alumina pans in a TA Instruments SDT Q600 analyzer. Samples for TGA were heated from room temperature to 1000 °C at 5 °C min⁻¹ in air. Nitrogen sorption isotherms and textural properties of the activated and compactivated carbons were determined at -196 °C using

nitrogen in a conventional volumetric technique by Micromeritics ASAP 2020 or 3FLEX sorptometers. Before their analysis, the carbons were dried in an oven at 120 °C and then degassed overnight at 200 °C under high vacuum. The surface area was calculated using the BET method based on adsorption data in the relative pressure (P/P_0) range of 0.05 to 0.22, and the relative pressure range was selected to ensure a positive y-axis intercept from multipoint BET fitting (such that $C > 0$) and that $V_{ads}(1 - p/p_0)$ would increase with p/p_0 .⁴⁶ The total pore volume was determined from the amount of nitrogen adsorbed at a relative pressure of ~ 0.99 . The pore size distribution (PSD) was determined using a Non Local Density Functional Theory (NLDFT) model using nitrogen adsorption data.

Gas uptake measurements

CO₂ uptake measurements were performed at 25 °C or 0 °C over the pressure range of 0 – 50 bar with a Hiden XEMIS intelligent gravimetric analyzer or at 0 – 20 bar with a Hiden intelligent gravimetric analyzer (IGA-003). The carbon samples were outgassed under vacuum at 200 °C before determining the CO₂ uptake isotherms. Buoyancy corrections were applied, and the measurements determined the excess CO₂ uptake from which the total storage capacity could be determined.

Hydrogen uptake capacity of the carbons was measured by gravimetric analysis with a Hiden XEMIS Intelligent Gravimetric Analyser using 99.9999% purity hydrogen additionally purified by a molecular sieve filter. Prior to analysis, the carbon samples were dried in an oven for 24 h at 80 °C and then placed in the analysis chamber and degassed at 200 °C and 10^{-10} bar for 4 – 6 h. The hydrogen uptake measurements were performed at room temperature (25 °C).

Results and Discussion

The aim of this study was to explore the preparation of super porous carbons at very high levels of activation and to assess their CO₂ uptake at high pressures that are relevant to pre combustion CCS. For this purpose we primarily used polypyrrole (PPy) as precursor as it is known to generate high surface area activated carbons that retain a high packing density.^{20,47} Following activation, we determined that the resulting PPy-derived activated carbons were fully carbonaceous by performing thermogravimetric analysis (TGA) in air. TGA curves of some representative samples (Supporting Figure S1) indicated residual mass of 0 – 1.5 wt%, which is normal for KOH activated carbons. The TGA curves also offered information on the thermal stability of the carbons; in general samples activated at higher activation temperature show greater resistance to combustion (Supporting Figure S1) perhaps due to higher levels of graphitisation induced during the thermal treatment. However, the overall level of graphitisation in the samples was generally low as indicated by powder XRD patterns (Supporting Figure S2). Low levels of graphitisation are conducive for the generation of high levels of porosity, which is a target in this work. The elemental composition of the polypyrrole and the activated carbons is given in Table 1. As expected, the carbon content increases at higher levels of activation accompanied by a decrease in the N, H and O content. It is noteworthy that, due to their high level of activation, the N content of the activated carbons is very low (i.e., 0.1 – 0.7 wt%). This is consistent with the fact that the N content of activated carbons prepared from N containing precursors generally reduces at high levels of activation.^{37,47} We monitored the yield of activated carbon as a function of the amount of polypyrrole and despite the elevated activation conditions, the yields were 11 – 21 wt%. Sample PPY-4700 had the highest yield (21 wt%), which decreased at higher levels of activation to ~ 11 wt% for sample PPY-4900 and PPY-5900. Such yields are typical for KOH activation and are higher than for activated carbons prepared via physical activation.^{20,47,48}

Table 1. Elemental composition of polypyrrole-derived activated (PPY-xT) carbons and compactivated (MPPY-4800) carbon.

Sample	C [%]	H [%]	N [%]	O [%]
PPY	54.8	3.2	16.0	26.0
PPY-4700	91.1	1.1	0.7	7.1
PPY-4800	93.7	0.4	0.5	5.4
MPPY-4800	94.0	0.3	0.4	5.3
PPY-5800	86.8	0	0.4	12.8
PPY-3900	92.1	0	0.4	7.7
PPY-4900	94.1	0	0.2	5.7
PPY-5900	88.7	0	0.1	11.2

The nitrogen sorption isotherms of the PPY-derived activated carbons are shown in Figure 1A. All the samples exhibit type IV isotherms that are typical of mesoporous materials. All isotherms also exhibit significant adsorption at low relative pressure ($P/P_0 < 0.1$), which is an indication that the present activated carbons possess high surface area despite their mesoporous character. The total amount of nitrogen adsorbed increases for samples prepared at higher temperature and/or higher KOH/PPy ratio in the order $PPY-4700 < PPY-4800 < PPY-3900 < PPY-5800 \sim PPY-4900 < PPY-5900$. As far as we know, polypyrrole-derived carbons have not previously been prepared via KOH activation at KOH/PPy ratio of 5 and/or 900 °C.^{20,47,48} The amount of nitrogen adsorbed is much higher than previously observed for activated carbons in general.^{20,47,48} The isotherms in Figure 1A suggest that the main effect of greater levels of activation and compactivation (MPPY-4800 compared to PPY-4800) is an increase in the porosity without any significant change in the shape of the isotherms except for sample PPY-5900, which is prepared at the severest conditions.

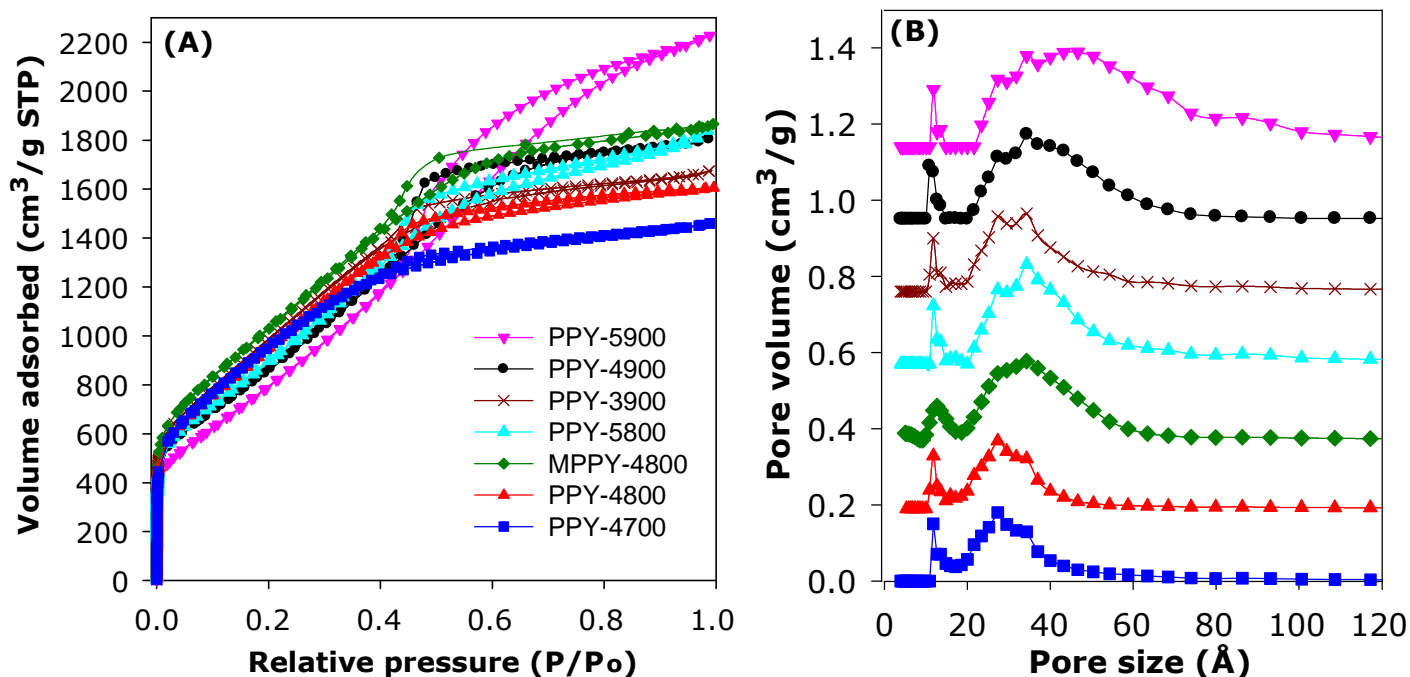


Figure 1. Nitrogen sorption isotherms (A) and corresponding pore size distribution (PSD) curves (B) of polypyrrole-derived (PPY-xT) activated carbons and compactivated (MPPY-4800) carbon.

The textural parameters and packing density of the activated and compactivated carbons are summarised in Table 2. All the carbons possess high or ultra-high surface area, which ranges between 2800 and 3940 m^2g^{-1} . In calculating the surface area, for all samples we confirmed that the data points used to determine the surface area gave a BET, or C, constant that is positive; this was evidenced by observing the Rouquerel plots and the value of the C constants (Supporting Figure S3). Apart from their high to ultra-high surface area, the carbons also possess high to very high pore volume in the range 2.45 – 3.60 cm^3g^{-1} . The highest surface area for an activated carbon is for PPY-4700 (3568 m^2g^{-1}) and PPY-4800 (3589 m^2g^{-1}), while samples PPY-5800 (2.85 cm^3g^{-1}) and PPY-5900 (3.54 cm^3g^{-1}) have the highest pore volume. Although all the activated carbons possess high porosity (i.e., surface area and pore volume), the balance between surface area and pore volume is such that the most highly activated carbons have the highest pore volume, but at the expense of a slight reduction in surface area (Table 2).

All the carbons have very low levels of microporosity such that the proportion of volume arising from mesopores (referred to as mesoporosity) is above 90% and up to 95% (Table 2). This means that the present carbons are essentially mesoporous in character. The porosity of the carbons may be improved via compactivation as demonstrated by comparison between the analogously activated (PPY-4800) and compactivated (MPPY-4800) samples. The activated PPY-4800 sample has surface area and pore volume of 3589 m²g⁻¹ and 2.71 cm³g⁻¹, respectively, compared to 3934 m²g⁻¹ and 2.92 cm³g⁻¹ for the compactivated MPPY-4800 sample. The compactivated MPPY-4800 carbon appears to have an optimised mix of ultra-high surface area, pore volume and high (93%) mesoporosity.

Table 2. Textural properties and packing density of polypyrrole-derived activated (PPY-xT) carbons and compactivated (MPPY-4800) carbon.

Sample	Surface area (m ² g ⁻¹)	Pore volume ^a (cm ³ g ⁻¹)	Pore size ^b (Å)	Mesoporosity ^c (%)	Packing density (g cm ⁻³)
PPY-4700	3568	2.46 (0.28)	27	89	0.34
PPY-4800	3589	2.71 (0.25)	28	91	0.32
MPPY-4800	3934	2.92 (0.20)	34	93	0.38
PPY-5800	2974	2.85 (0.22)	35	92	0.30
PPY-3900	3285	2.60 (0.30)	32	88	0.33
PPY-4900	2842	2.77 (0.27)	36	90	0.31
PPY-5900	2798	3.54 (0.19)	46	95	0.25

^aThe values in the parenthesis are micropore volume. ^bmain pore size maxima obtained from NLDFT analysis. ^cProportion of pore volume arising from mesopores.

The mesoporous nature of the activated carbons and compactivated carbon is confirmed by the pore size distribution (PSD) curves in Figure 1B. For all samples, the main pore size maxima is in the mesopore range of 27 to 46 Å. In general, the main pore size maxima increases with the severity of activation such that the sample prepared under the most severe conditions

(PPY-5900) has the largest mesopores (46 Å). Table 2 gives the packing density of the carbons, which varies between 0.25 and 0.38 g cm⁻³. The packing density of the compactivated carbon (MPPY-4800) and some of the activated carbons was determined by pressing a known amount of sample in a 1.3 cm die at pressure of 74 MPa for 5 min. Such compaction has no effect on the porosity of the carbons.²⁰ For activated carbons, the packing density (d_{carbon}) may also be estimated from skeletal density using the equation; $d_{\text{carbon}} = (1/\rho_s + V_T)^{-1}$, where ρ_s is skeletal density and V_T is total pore volume. The skeletal density used (2.1 g cm⁻³) was obtained from helium sorption at 0 °C. There is an inverse relationship between the total pore volume and the packing density of the activated carbons. The compactivated carbon bucks this trend as it was already compacted prior to activation and therefore has a higher than expected packing density.²⁰ Overall, therefore, with respect to porosity, we succeeded in generating mesoporous carbons with simultaneously high surface area and pore volume. In particular, the present carbons have very low levels of microporosity which is unusual for high surface area activated carbons.³⁷⁻⁴⁹ The near elimination of microporosity is achieved by choice of precursor and activation conditions.^{20,37-49}

We assessed the CO₂ uptake capacity of the activated carbons at room temperature (25 °C) and pressure range of 0 to 50 bar. The main focus was the CO₂ uptake at moderate to high pressure (20 – 50 bar) under conditions that attempt to mimic pre combustion CCS. The total gravimetric CO₂ uptake isotherms are shown in Figure 2. Our measurements determined the excess CO₂ uptake (Supporting Figure S4) from which the total storage capacity was obtained by considering the density of the CO₂ under the prevailing conditions and the carbon's pore volume using the equation; $\theta_T = \theta_{Exc} + d_{\text{CO}_2} \times V_T$, where; θ_T is total CO₂ uptake, θ_{Exc} is excess CO₂ uptake, d_{CO_2} is density (g cm⁻³) of CO₂ gas at the relevant temperature and pressure (the density of CO₂ was obtained from the National Institute of Standards and Technology (NIST) website (<http://www.nist.gov/>)), and V_T is pore volume (cm³g⁻¹) of the carbon. Table 3

summarizes the amount of CO₂ adsorbed at various pressures. At 1 bar, the CO₂ uptake is in the range 1.3 – 2.8 mmol g⁻¹, which is low or moderate capacity compared to benchmark carbon materials.^{11-14,20-37} The storage capacity at 1 bar is consistent with the well-established fact that it is not the total surface area or pore volume, but the pore size that determines the CO₂ uptake at low pressure.¹¹⁻³⁷ On the other hand, the CO₂ uptake increases continuously at higher pressures to reach very high levels of storage at 50 bar. For all samples the CO₂ uptake was fully reversible with no hysteresis, and no saturation was attained in the 0 – 50 bar pressure range except for sample PPY-4700 (Figure 2 and Supporting Figure S4). At 20 bar the PPY-derived carbons store between 23 and 28 mmol g⁻¹, with excess uptake in the range 20.6 – 25.5 mmol g⁻¹. This uptake is much higher than that previously reported for any carbon material.^{11-14,20-37} At 30 bar the CO₂ storage capacity rises to between 29.6 and 37.7 mmol g⁻¹, with excess uptake in the range 26.0 – 33.0 mmol g⁻¹. This is higher than the current benchmark carbons, namely, polyaniline cross-linked polymer networks (SU-AC-400) that store 28.3 mmol g⁻¹ under similar conditions (i.e., 25 °C and 30 bar).³⁸ At 50 bar, which is the highest pressure used in this study, the carbons have exceptionally high CO₂ storage capacity of 40 to 55 mmol g⁻¹, with excess uptake in the range 33.0 – 45.4 mmol g⁻¹. Total CO₂ uptake of 55 mmol g⁻¹ is exceptionally high and in any case is significantly greater (higher by ca. 60%) than that (34.9 mmol g⁻¹) reported recently for polyaniline cross-linked polymer networks (SU-AC-400)³⁸ or that (35.2 mmol g⁻¹) for asphalt-derived carbon (UGil-900).³⁹ The gravimetric CO₂ uptake at high pressure (20 – 50 bar) closely matches the trend in pore volume such that the best performing samples (PPY-5900 and MPPY-4800) also have both the highest pore volume and highest levels of mesoporosity (93 – 95%). Comparison between PPY-4800 and MPPY-4800 illustrates how compaction²⁰ may be used to significantly enhance the porosity of activated carbons and consequently their CO₂ uptake under conditions that are relevant to pre combustion CCS.

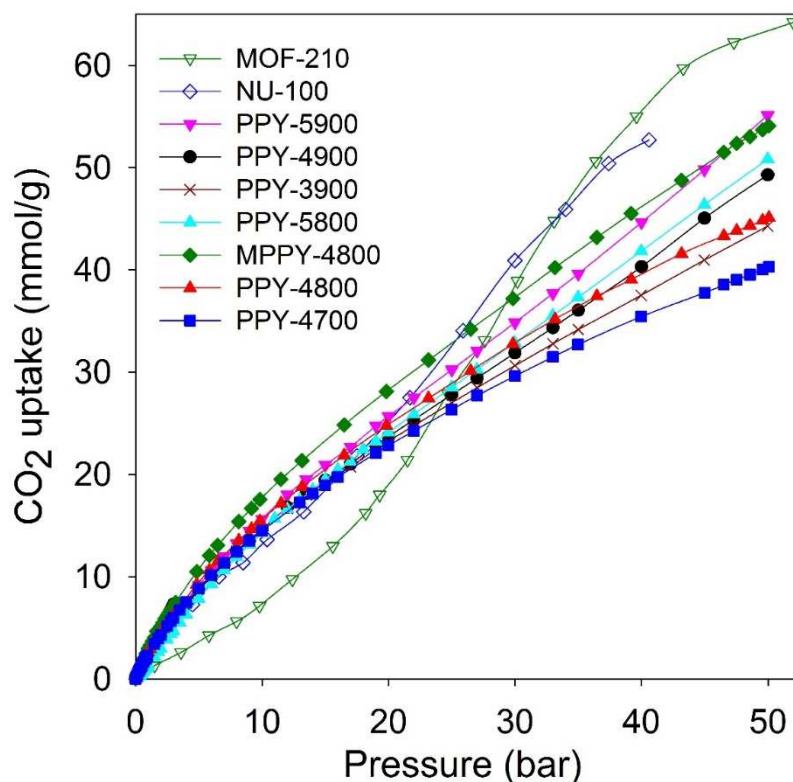


Figure 2. Total gravimetric CO₂ uptake at 25 °C of polypyrrole-derived activated (PPY-xT) carbons, a compactivated (MPPY-4800) carbon and MOFs (MOF-210 and NU-100).

Table 3. Total and excess gravimetric CO₂ uptake of polypyrrole-derived activated (PPY-xT) carbons, a compactivated (MPPY-4800) carbon and MOFs (MOF-210 and NU-100).

Sample	CO ₂ uptake ^a (mmol g ⁻¹)				
	1 bar	20 bar	30 bar	40 bar	50 bar
PPY-4700	2.3	22.8 (20.6)	29.6 (26.0)	35.4 (30.2)	40.3 (32.9)
PPY-4800	2.5	25.0 (22.5)	33.0 (29.0)	39.5 (34.0)	45.3 (37.2)
MPPY-4800	2.8	28.1 (25.5)	37.2 (33.0)	45.6 (39.5)	54.1 (45.4)
PPY-5800	1.3	24.1 (21.5)	32.8 (28.7)	41.8 (35.8)	50.8 (42.3)
PPY-3900	2.2	23.2 (20.9)	30.7 (26.9)	37.5 (32.0)	44.5 (36.5)
PPY-4900	2.0	23.6 (21.2)	31.9 (27.9)	41.4 (34.4)	49.3 (41.0)
PPY-5900	2.1	25.7 (22.5)	34.9 (29.7)	44.6 (37.1)	55.1 (44.5)
MOF-210	0.9	19.2 (16.0)	38.9 (33.7)	55.0 (46.7)	64.2 (52.5)
NU-100	2.7	24.6 (22.0)	40.9 (36.3)	52.7 (46.8)	

^aCO₂ uptake at 25 °C and various pressures (i.e., 1, 20, 30, 40 and 50 bar). The values in the parenthesis are excess CO₂ uptake.

The gravimetric CO₂ uptake of the present PPy-derived carbons compares favourably (Figure 2, Supporting Figure S4 and Supporting Table S1 and S2) with that of the best performing high surface area metal organic frameworks (MOFs), namely, NU-100,⁵⁰ and MOF-210,⁵¹ which are the current record holders with respect to gravimetric CO₂ storage at ambient temperature and high pressure.⁵² It is noteworthy that the total gravimetric CO₂ uptake of samples PPY-5900 and MPPY-4800 at 50 bar is similar to that of NU-100.⁵⁰ This finding demonstrates the importance of the pore volume (and in particular the mesopore volume) in determining the high pressure CO₂ uptake; for example although the surface area of NU-100 (6143 m²g⁻¹) is more than twice that of PPY-5900 (2798 m²g⁻¹), the two samples have similar high pressure CO₂ uptake (Figure 2) on account of their comparable *mesopore volume* (Table 2 and 3 and Supporting Table S1 and S2).

To further illustrate the importance of mesopore volume, we compared the CO₂ uptake of the PPy-derived carbons to that of activated carbons that have similarly high surface area but lower levels of mesoporosity (Table S1 and S2). Comparison with a highly microporous carbon (designated as CA-4700) derived from activation of hydrochar of cellulose acetate (at 700 °C and KOH/hydrochar ratio of 4) is very revealing. Sample CA-4700 presents a type 1 nitrogen sorption isotherm (Supporting Figure S5) and has surface area of 3771 m²g⁻¹ (with 3484 m²g⁻¹, i.e., 92% arising from micropores), pore volume of 1.75 cm³g⁻¹ and micropore volume of 1.54 cm³g⁻¹. Sample CA-4700, therefore, has mesopore volume of only 0.21 cm³g⁻¹ and a mesoporosity level of 12% (Table S1). In line with its microporous nature, sample CA-4700 has high CO₂ uptake (i.e., 3.7 mmol g⁻¹) at 1 bar, which is higher than that of the mesoporous PPy-derived carbons (Supporting Figure S6 and S7, and Table S2). However, at 20 bar, total CO₂ uptake by the mesoporous PPy-derived samples (23 – 28 mmol g⁻¹) far outperforms the microporous CA-4700 sample (19.5 mmol g⁻¹). Furthermore, in the 20 – 50 bar pressure range, there is very little increase in the excess storage capacity of sample CA-4700; uptake increases

from 18.0 to 20.5 mmol g⁻¹, a rise of only 6% (Figure S6 and Table S2). On the other hand, the excess CO₂ uptake of PPy-derived carbons nearly doubles from 21 – 26 mmol g⁻¹ to a high of 45 mmol g⁻¹ as pressure rises from 20 to 50 bar (Figure S6 and Table S2). A similar trend is observed in the total CO₂ uptake within the 20 – 50 bar pressure range (Figure S7 and Table S2). We attribute this stark difference in CO₂ uptake behaviour between CA-4700 and the PPy-derived carbons (Supporting Figure S6 and S7) to differences in mesoporosity, and especially the balance between microporosity and mesoporosity. This conclusion is supported by the fact that activated carbon samples (AC-0 and AC-2M),³⁷ with mesoporosity that is intermediate between the PPy-derived carbons and CA-4700 (Table S1) also show intermediate CO₂ uptake (Supporting Figure S8 and Table S2) at high pressure (20 – 50 bar). This confirms that mesoporosity favours high pressure CO₂ uptake while the presence of micropores can be a limiting factor.

A key measure of the efficiency of an adsorbent for pre combustion CCS is the working capacity, which is the difference in CO₂ uptake between the adsorption and desorption (regeneration) pressure. For desorption at atmospheric pressure (1 bar), a microporous carbon such as CA-4700 has pressure swing adsorption (PSA) working capacity (in mmol g⁻¹) of 16 (20 bar), 19 (30 bar), 20 (40 bar) and 22 (50 bar). For the mesoporous carbons, the working capacity vastly increases up to 25 (20 bar), 33 (30 bar), 43 (40 bar) and 53 (50 bar), wherein it is more than twice that of the microporous CA-4700 at 40 bar and above. Such working capacity is superior to that of all previously reported carbons.^{13,37-39,53-56}

The PPy-derived carbons have very low N-content (Table 1), which means that their exceptional CO₂ uptake may not be ascribed to N-doping. However, to ascertain that N-doping does not play a key role, and also to test the general applicability of the link between high mesoporosity and high pressure CO₂ uptake, we prepared and analysed an activated carbon (designated as SD-4800) and compactivated carbon (designated as MDS-4800) derived from

wood sawdust as precursor and prepared at a KOH/carbon ratio of 4 at 800 °C. The nitrogen sorption isotherms of both sawdust derived carbons (Figure 3) are type IV with much higher nitrogen adsorption for the compactivated carbon (MSD-4800). The activated (SD-4800) and compactivated (MSD-4800) carbons have surface area of 2790 m²g⁻¹ and 3982 m²g⁻¹, respectively (Table 4). The pore volume is 1.77 cm³g⁻¹ (SD-4800) and 2.56 cm³g⁻¹ (MSD-4800) with micropore volume of 0.35 (SD-4800) and 0.28 cm³g⁻¹ (MSD-4800), and mesoporosity of 80% and 89%, respectively (Table 4). As shown in Figure 4, both samples, and in particular MSD-4800, have high CO₂ uptake at 25 °C, which is comparable to that of PPy-derived carbons. The sawdust-derived samples also show excellent storage of up to 33 mmol g⁻¹ (SD-4800) and 37.5 mmol g⁻¹ (MSD-4800) at 0 °C and 20 bar (Supporting Figure S9). The CO₂ uptake of these N-free samples indicates that it is primarily the optimised *mesoporosity* that is responsible for the high uptake rather than the presence or absence of N.

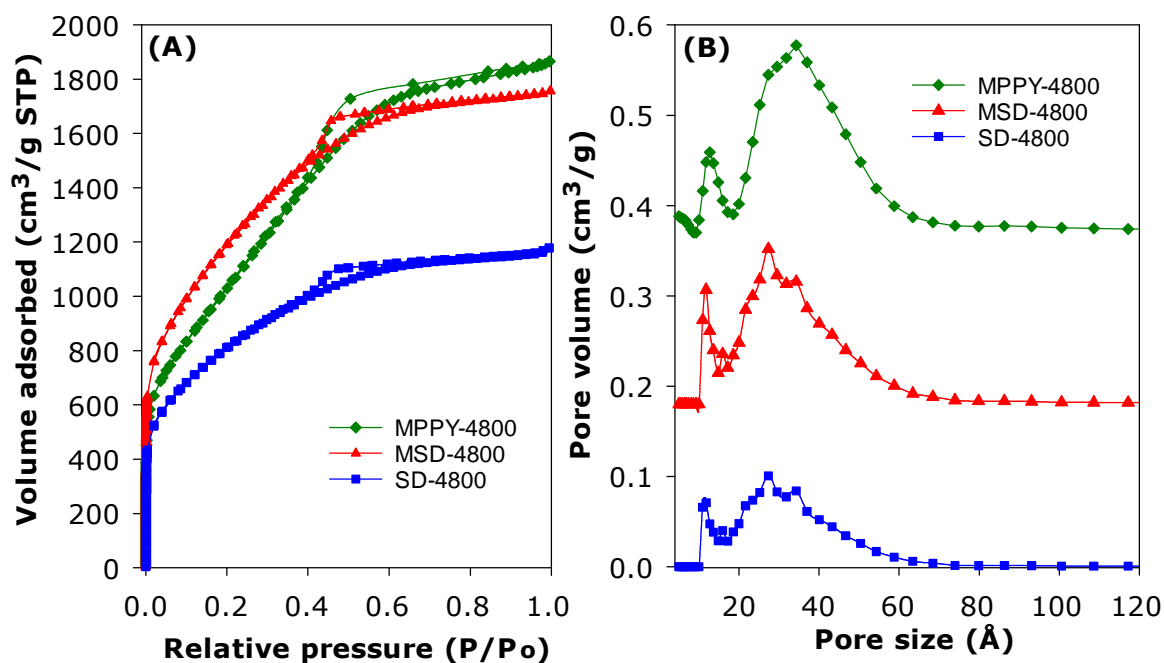


Figure 3. Nitrogen sorption isotherms (A) and corresponding pore size distribution (PSD) curves (B) of polypyrrole-derived compactivated carbon (MPPY-4800), and an activated (SD-4800) or compactivated (MSD-4800) carbon derived from wood sawdust.

Table 4. Textural properties and CO₂ uptake of activated (SD-4800) and compactivated (MSD-4800) carbon derived from wood sawdust.

Sample	Surface area (m ² g ⁻¹)	Pore volume ^a (cm ³ g ⁻¹)	Pore size ^{b,c} (Å)	CO ₂ uptake ^{d,e} (mmol g ⁻¹)				
				1 bar	20 bar	30 bar	40 bar	50 bar
SD-4800	2790	1.77 (1.42)	28 (80)	2.9	22.8 (21.0)	29.7 (27.1)	35.4 (31.6)	40.2 (34.8)
MSD-4800	3982	2.56 (2.28)	31 (89)	2.7	26.3 (24.0)	34.8 (31.0)	42.5 (37.5)	50.4 (42.8)

^aThe values in the parenthesis refer to mesopore volume. ^bmain pore size distribution maxima obtained from NLDFT analysis. ^cThe values in the parenthesis are % mesoporosity. ^dtotal CO₂ uptake at 25 °C and various pressures. ^eThe values in the parenthesis are excess CO₂ uptake..

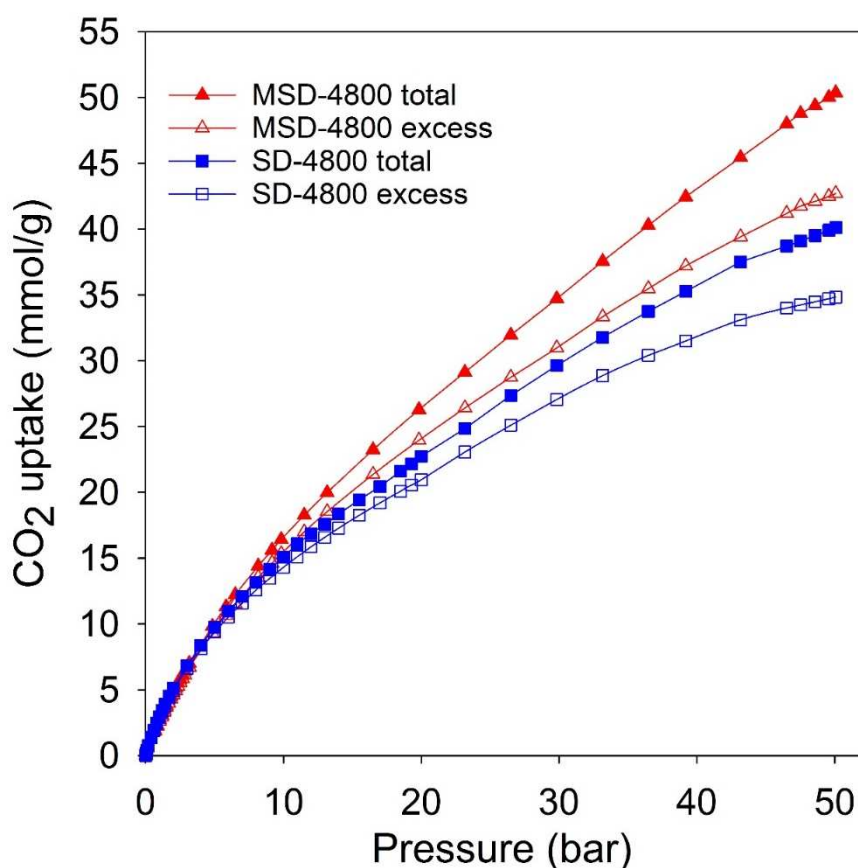


Figure 4. Total and excess CO₂ uptake at 25 °C and 0 – 50 bar of activated (SD-4800) and compactivated (MSD-4800) carbon derived from wood sawdust.

The foregoing discussion indicates that the present mesoporous carbons have exceptional gravimetric CO₂ uptake. However, of equal or even greater importance is the volumetric CO₂ uptake. This is because for pre combustion CCS applications the adsorbent is confined in restricted space such as a high pressure tank, and therefore the CO₂ stored per given volume occupied by the adsorbent (i.e. volumetric uptake) is a key consideration. The volumetric gas uptake of porous materials is determined by their packing density, and gravimetric storage capacity. The PPy-derived carbons have packing density of 0.25 – 0.38 g cm⁻³ (Table 2). The volumetric CO₂ uptake of the carbons is shown in Figure 5 (and supporting Figure S10) and the capacity at various pressures is summarised in Table 5. At 20 bar the mesoporous carbons store an impressive 280 to 480 g l⁻¹, with excess uptake of 240 – 440 g l⁻¹. At 30 bar the capacity rises to between 380 and 640 g l⁻¹, with excess uptake in the range 327 – 566 g l⁻¹ while at 40 bar it is between 490 and 780 g l⁻¹, with excess uptake in the range 408 – 680 g l⁻¹. The volumetric uptake increases steadily at higher pressure and at 50 bar is exceptionally high; 600 to 940 g l⁻¹, with excess uptake in the range 490 – 780 g l⁻¹. Such high volumetric CO₂ storage capacity is, to the best of our knowledge, the highest reported so far for any porous material. The volumetric uptake is much higher than that of high surface area metal organic framework materials, MOF210 and NU-100 (Figure 5, Table 5 and Figure S10), which have uptake of, respectively; 90 and 165 g l⁻¹ (20 bar), 190 and 270 g l⁻¹ (30 bar), 270 and 350 g l⁻¹ (40 bar), and 311 for MOF-210 at 50 bar. This means that the volumetric CO₂ uptake of the mesoporous carbons is consistently 2 to 3 times higher than that of the benchmark MOFs. It is noteworthy that the mesoporous carbons still outperform MOFs even when crystal density (rather than packing density) is used to compute the volumetric CO₂ uptake of MOF-210 and NU-100 (Supporting Figure S11). The use of crystal density to estimate volumetric uptake is known to generate overestimated values and is not realistic for scenarios where the MOFs are packed into constrained space such as a cylinder.^{46,57-61}

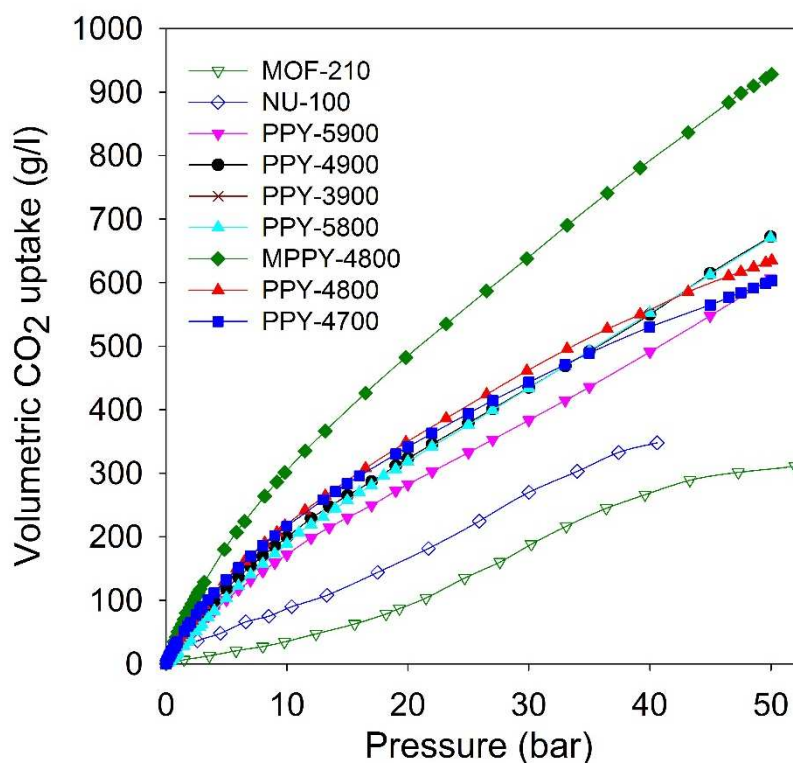


Figure 5. Total volumetric CO₂ uptake at 25 °C of polypyrrole-derived activated (PPY-xT) carbons, compactivated (MPPY-4800) carbon and MOFs (MOF-210 and NU-100).

Table 5. Total and excess volumetric CO₂ uptake of polypyrrole-derived activated (PPY-xT) carbons and compactivated (MPPY-4800) carbon and MOFs (MOF-210 and NU-100).

Sample	CO ₂ uptake ^a (g l ⁻¹)				
	1 bar	20 bar	30 bar	40 bar	50 bar
PPY-4700	34	341 (308)	443 (389)	530 (452)	603 (492)
PPY-4800	35	352 (317)	465 (408)	556 (479)	638 (524)
PPY-5800	17	318 (284)	433 (379)	552 (473)	671 (558)
PPY-3900	33	338 (303)	445 (390)	545 (465)	643 (530)
PPY-4900	27	322 (289)	435 (381)	565 (469)	672 (559)
PPY-5900	23	282 (247)	383 (327)	491 (408)	606 (490)
MPPY-4800	48	482 (438)	638 (566)	783 (678)	928 (780)
MOF-210 ^c	4	93 (77)	188 (163)	266 (226)	311 (254)
NU-100 ^c	18	163 (145)	270 (240)	348 (309)	

^aCO₂ uptake at 25 °C and various pressures (i.e., 1, 20, 30, 40 and 50 bar). The values in the parenthesis are excess CO₂ uptake. ^cPacking density values (g cm⁻³) used are: 0.15 (NU-100) and 0.12 (MOF-210).⁵⁶ MOF data adapted from reference 50 and 51.

The volumetric uptake may also be expressed per volume occupied by the adsorbent. This is especially useful for high pressure pre combustion CCS as it enables easy assessment of an adsorbent's uptake capacity in comparison with an empty cylinder of equal volume. The volumetric capacity of the mesoporous carbons (expressed as $\text{cm}^3 \text{cm}^{-3}$) as a function of pressure is shown in Figure 6. The uptake is in the order pressurized CO_2 < MOFs < activated (PPY-xT) carbons < compactivated (MPPY-4800) carbon. At 20 bar and 25 °C, pressurised CO_2 equates to $20 \text{ cm}^3 \text{cm}^{-3}$ while MOFs store 47 and $83 \text{ cm}^3 \text{cm}^{-3}$ for MOF-210 and NU-100, respectively. On the other hand, PPY-xT activated carbons store 144 to $178 \text{ cm}^3 \text{cm}^{-3}$, and an impressive 246 for the compactivated carbon (MPPY-4800). At 30 bar the volumetric capacity of the mesoporous carbons rises to between 195 and $325 \text{ cm}^3 \text{cm}^{-3}$, compared to $95 - 137 \text{ cm}^3 \text{cm}^{-3}$ (MOFs) and $33 \text{ cm}^3 \text{cm}^{-3}$ for pressurized CO_2 . Thus at 30 bar, the present mesoporous carbons can enable CO_2 storage at twice the capacity of MOFs and 10 times that of an empty cylinder. The volumetric uptake of the mesoporous carbons reaches, at 50 bar, exceptionally high capacity of between 310 and $470 \text{ cm}^3 \text{cm}^{-3}$, compared to $158 \text{ cm}^3 \text{cm}^{-3}$ for MOF-210 and $67 \text{ cm}^3 \text{cm}^{-3}$ for pressurized CO_2 .

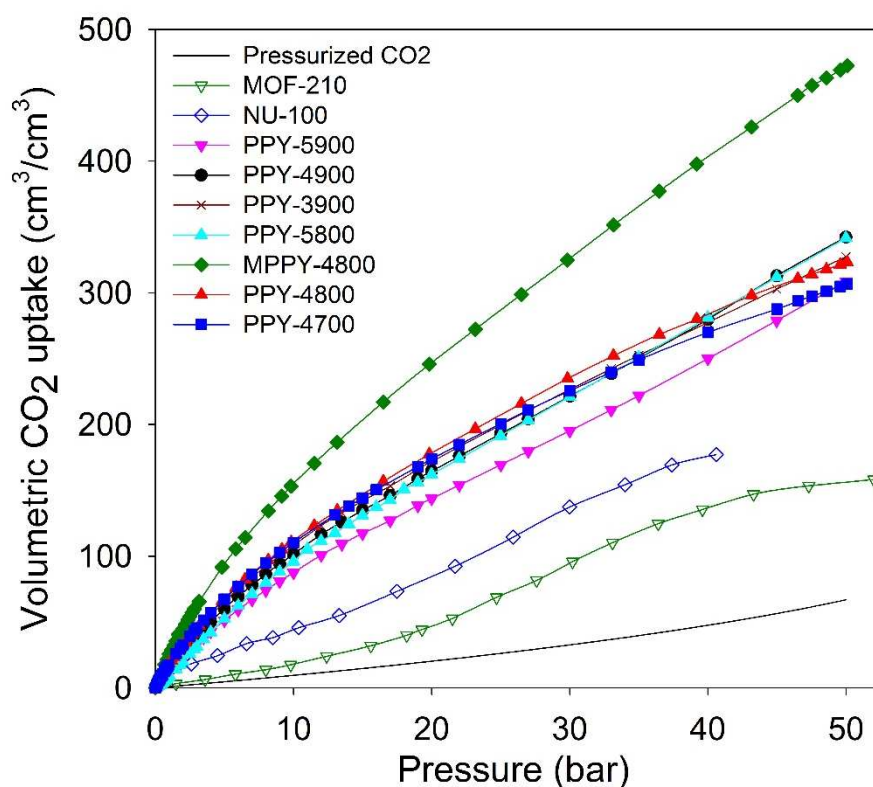


Figure 6. Total volumetric CO₂ uptake at 25 °C of polypyrrole-derived activated (PPY-xT) carbons, compactivated (MPPY-4800) carbon and MOFs (MOF-210 and NU-100).

The exceptional uptake of the present mesoporous carbons suggests that they may be suitable materials for the removal of CO₂ from syngas during which the H₂ content is enriched. Syngas, which is a fuel for energy generation from power stations typically contains 71–75% H₂, 15–20% CO₂, and ca. 5% of other gases (CH₄, CO, H₂O). We therefore compared the high pressure CO₂ uptake with the H₂ adsorption capacity for one of the best performing mesoporous carbons (MPPY-4800) so as to determine the selectivity for CO₂. The selectivity for CO₂ was also estimated for CO₂/H₂ mixtures with composition similar to that of syngas. We compared the performance of MPPY-4800 with that of a microporous carbon (CA-4700) of similar surface area. The excess CO₂ and H₂ uptake of mesoporous MPPY-4800 and microporous CA-4700 are shown in Figure 7. For both samples, the CO₂ uptake is much higher than the H₂ uptake. There are, however, important differences in the CO₂/H₂ uptake ratio for the two

samples that highlight the role played by mesoporosity in determining the relative adsorption of the two gases and thus the preference for CO₂. Figure 8A shows plots of the equilibrium CO₂/H₂ adsorption ratio for the two samples as a function of uptake pressure. At low pressure (1 bar), the microporous carbon (CA-4700) has a higher CO₂/H₂ ratio (10.2) compared to the mesoporous MPPY-4800 (7.8) due to a greater CO₂ uptake arising from the presence of micropores in the former. However at higher pressures (> 5 bar) that are more relevant to syngas purification, the CO₂/H₂ ratio for the mesoporous carbon increases significantly, while that of the microporous carbon drops drastically (Figure 8A). Comparison of the relative excess uptake of CO₂ and H₂ at 50 bar indicates that CO₂ uptake of MPPY-4800 (45.4 mmol g⁻¹) is far higher than that of H₂ (4.13 mmol g⁻¹). Thus the equilibrium CO₂/H₂ adsorption ratio (at 50 bar) for MPPY-4800 is high at 11. For the microporous sample (CA-4700) the CO₂ uptake at 50 bar is 20.5 mmol g⁻¹ while for H₂ it is 5.4 mmol g⁻¹, giving an equilibrium CO₂/H₂ adsorption ratio of 3.8. The mesoporous carbon is therefore better suited for H₂ purification under syngas flow conditions.

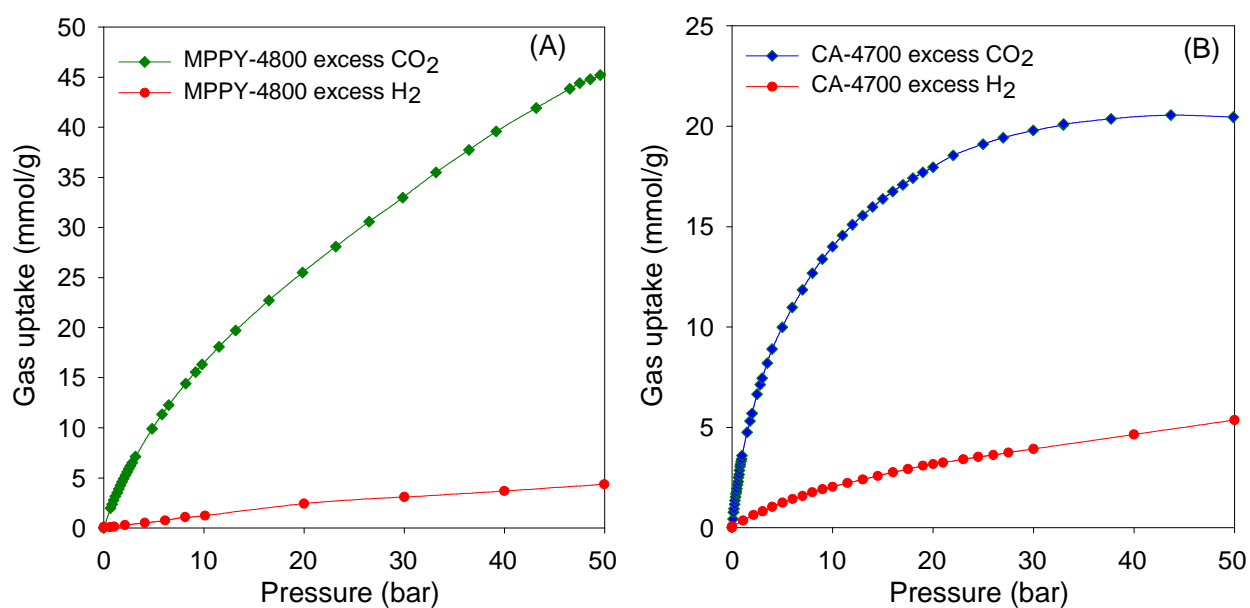


Figure 7. Comparison of excess CO₂ and H₂ uptake isotherms at room temperature for (A) mesoporous carbon (MPPY-4800) and (B) microporous carbon (CA-4700).

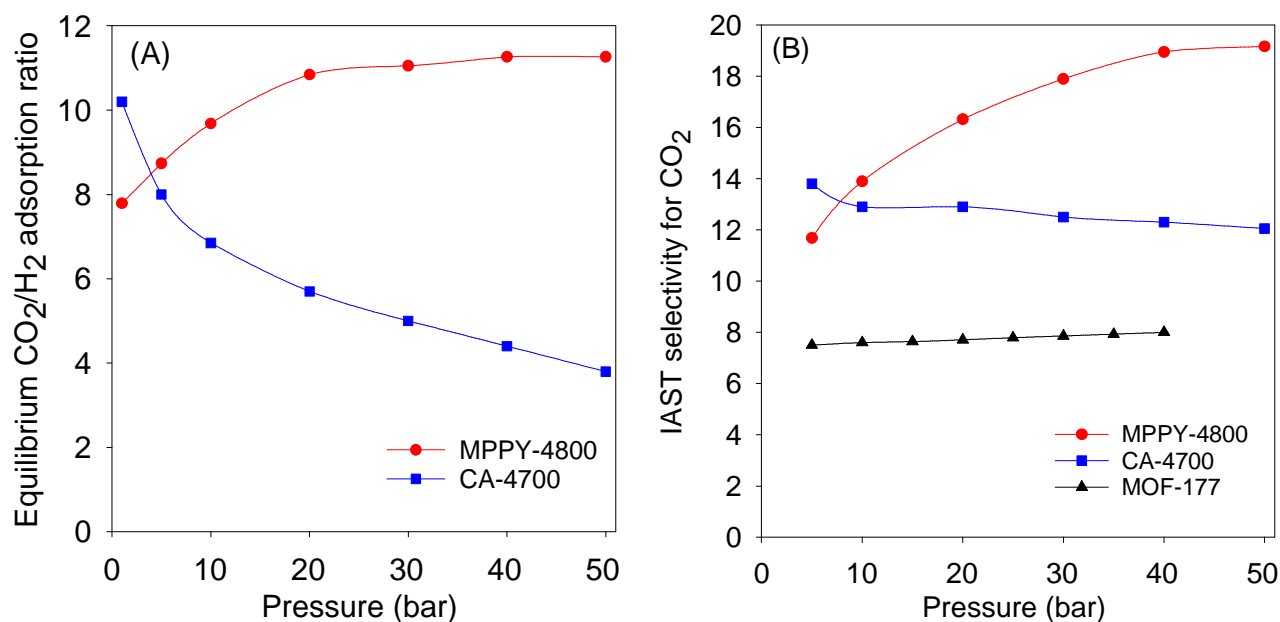


Figure 8. (A) Equilibrium CO₂/H₂ adsorption ratio as a function of uptake pressure at 25 °C, and (B) IAST CO₂/H₂ selectivity for a 80:20 H₂/CO₂ mixture at 25 °C for mesoporous (MPPY-4800) carbon, microporous (CA-4700) carbon and a metal organic framework (MOF-177). Data for MOF-177 was obtained from reference 61.

The selectivity for CO₂ adsorption may also be estimated from a simulated pre combustion syngas stream with a 80:20 H₂/CO₂ mixture. The simulation is based on the fact that syngas streams typically contain 71–75% H₂ and 15–20% CO₂ and thus comparison of the CO₂ uptake from a 80:20 H₂/CO₂ mixture gives a realistic estimation of selectivity for CO₂. The selectivity analysis was determined using the ideal adsorbed solution theory (IAST) model, which is commonly applied in calculating the relative uptake of adsorbents for any two gases in a binary gas mixture.^{61,62} According to the IAST model, the selectivity (S) for CO₂ was derived from the following equation; $S = \frac{n(\text{CO}_2) p(\text{H}_2)}{n(\text{H}_2) p(\text{CO}_2)}$, where n is uptake of CO₂ and H₂ in mmol g⁻¹ at partial pressure of 0.2 and 0.8 bar, respectively, p(H₂) is 0.8 and p(CO₂) is 0.2. Figure 8B shows plots of the IAST selectivity for CO₂ as a function of uptake pressure. At 5 bar, the microporous carbon (CA-4700) has slightly higher IAST CO₂ selectivity

(13.8) compared to the mesoporous MPPY-4800 (11.7). However at higher pressures (> 5 bar) that are more relevant to syngas purification, the IAST CO_2 selectivity of the mesoporous carbon increases significantly to ≥ 18 at 40 bar and above. In contrast that of the microporous carbon drops to 12.0 – 12.5 at 20 to 50 bar (Figure 8A). The IAST CO_2 selectivity, therefore, demonstrates a clear advantage for the mesoporous carbons with respect to CO_2 removal from syngas. Furthermore, as shown in Figure 8B, the CO_2 selectivity of the mesoporous carbon is higher than that of a metal organic framework (MOF-177) that has similar surface area.⁶¹ The mesoporous carbons, due to their large mesopore volume and high surface area, appear to have very high affinity for CO_2 storage at pre combustion CCS conditions. The carbons fulfill the adsorbent requirements for syngas (or H_2) purification, namely, high CO_2 adsorption capacity and selectivity for CO_2 over H_2 .

Conclusions

In summary, we have described a new family of ultra-high surface area mesoporous carbons that possess extremely high mesopore volume with hardly any micropores present. The mesoporous carbons have surface area and pore volume in the range of $2800 - 4000 \text{ m}^2\text{g}^{-1}$ and $2.5 - 3.6 \text{ cm}^3\text{g}^{-1}$, respectively. The porosity of the carbons can be readily tailored by choice of the activation temperature and the amount of activator used. The mesoporosity of the carbons is found to be ideal for CO_2 uptake under conditions that closely mimic pre combustion carbon capture and storage, i.e., $25 \text{ }^\circ\text{C}$ and pressure of 20 to 50 bar. The best performing carbons are found to be those that have a near total absence of micropores; microporosity appears to limit high pressure CO_2 uptake. The gravimetric (mmol g^{-1}) CO_2 uptake capacities; up to 28 (20 bar), 37 (30 bar), 46 (40 bar) and 55 (50 bar), are among the highest ever reported for porous carbons. The high gravimetric CO_2 uptake of the mesoporous carbons in combination with their packing density ($0.25 - 0.4 \text{ g cm}^{-3}$) results in colossal volumetric uptake (in g l^{-1}) of up to 480 (20 bar),

640 (30 bar), 780 (40 bar) and 930 (50 bar). At 30 bar, the mesoporous carbons can hold more than 10 times the CO₂ in a pressurized cylinder, and at 50 bar can store up to 470 cm³ cm⁻³. We have shown that the all-round pre combustion CO₂ capture performance (gravimetric and volumetric uptake, and selectivity for CO₂) of the mesoporous carbons is significantly higher than that of the best carbons to date, and outperforms that of benchmark MOF materials. Due to their mesoporosity, the carbons are highly suited, in terms of the CO₂ adsorption capacity and selectivity over H₂, as materials for hydrogen purification under syngas flow conditions.

Acknowledgements: This research was funded by the University of Nottingham.

Supporting Information Available: Two (2) tables and eleven (11) figures.

References

1. M. E. Boot-Handford, J. C. Abanades, E. J. Anthony, M. J. Blunt, S. Brandani, N. Mac Dowell, J. R. Fernández, M.-C. Ferrari, R. Gross, J. P. Hallett, R. S. Haszeldine, P. Heptonstall, A. Lyngfelt, Z. Makuch, E. Mangano, R. T. J. Porter, M. Pourkashanian, G. T. Rochelle, N. Shah, J. G. Yao and P. S. Fennell. *Energy Environ. Sci.*, 2014, **7**, 130.
2. K. Z. House, A. C. Baclig, M. Ranjanc, E. A. van Nierop, J. Wilcox, and H. J. Herzog, *Proc. Nat. Acad. Sci.*, 2011, **108**, 20428.
3. S. Choi, J. H. Drese and C. W. Jones, *ChemSusChem*, 2009, **2**, 796.
4. H. J. Schellnhuber, *Proc. Nat. Acad. Sci.*, 2011, **108**, 20277.
5. K. S. Lackner, S. Brennan, J. M. Matter, A.-H. A. Park, A. Wright and B. van der Zwaan, *Proc. Nat. Acad. Sci.*, 2012, **109**, 13156.

6. T. C. Drage, C. E. Snape, L. A. Stevens, J. Wood, J. Wang, A. I. Cooper, R. Dawson, X. Guo, C. Satterley and R. Irons, *J. Mater. Chem.*, 2012, **22**, 2815.
7. G. T. Rochelle, *Science*, 2009, **325**, 1652.
8. S. Wang, S. Yan, X. Ma and J. Gong, *Energy Environ. Sci.*, 2011, **4**, 3805.
9. Q. Wang, J. Luo, Z. Zhong and A. Borgna, *Energy Environ. Sci.*, 2011, **4**, 42.
10. A. Samanta, A. Zhao, G. K. H. Shimizu, P. Sarkar and R. Gupta, *Ind. Eng. Chem. Res.*, 2012, **51**, 1438.
11. J. P. Marco-Lozar, M. Kunowsky, F. Suarez-Garcia, J. D. Carruthers and A. Linares-Solano, *Energy Environ. Sci.*, 2012, **5**, 9833.
12. G.-P. Hao, W.-C. Li, D. Qian and A.-H. Lu, *Adv. Mater.*, 2010, **22**, 853.
13. J. Silvestre-Albero, A. Wahby, A. Sepulveda-Escribano, M. Martinez-Escandell, K. Kaneko and F. Rodriguez-Reinoso, *Chem. Commun.*, 2011, **47**, 6840.
14. M. Sevilla and A. B. Fuertes, *J. Colloid Interface Sci.*, 2012, **366**, 147.
15. M. R. Hudson, Q. L. Queen, J. A. Mason, D. W. Fickel, R. F. Lobo, C. M. Brown, *J. Am. Ceram. Soc.*, 2012, **134**, 1970.
16. J. Mere, M. Clause and F. Meunier, *Ind. Eng. Chem. Res.*, 2008, **47**, 1209.
17. R. V. Siriwardane, M. S. Shen, E. P. Fisher and J. Losch, *Energy Fuels*, 2005, **19**, 1153.
18. Z. J. Zhang, Z. Z. Yao, S. C. Xiang and B. L. Chen, *Energy Environ. Sci.*, 2014, **7**, 2868.
19. K. Sumida, D. L. Rogow, J. A. Mason, T. M. McDonald, E. D. Bloch, Z. R. Herm, T.-H. Bae and J. R. Long, *Chem. Rev.*, 2012, **112**, 724.
20. B. Adeniran and R. Mokaya, *Nano Energy*, 2015, **16**, 173.
21. N. Balahmar, A. C. Mitchell, and R. Mokaya, *Adv. Energy Mater.*, **2015**, *5*, 1500867
22. W. Sangchoom and R. Mokaya, *ACS Sust. Chem. Eng.*, 2015, **3**, 1658.
23. A. Almasoudi and R. Mokaya, *J. Mater. Chem. A*, 2014, **2**, 10960.
24. C. Robertson and R. Mokaya, *Micropor. Mesopor. Mater.*, 2013, **179**, 151.

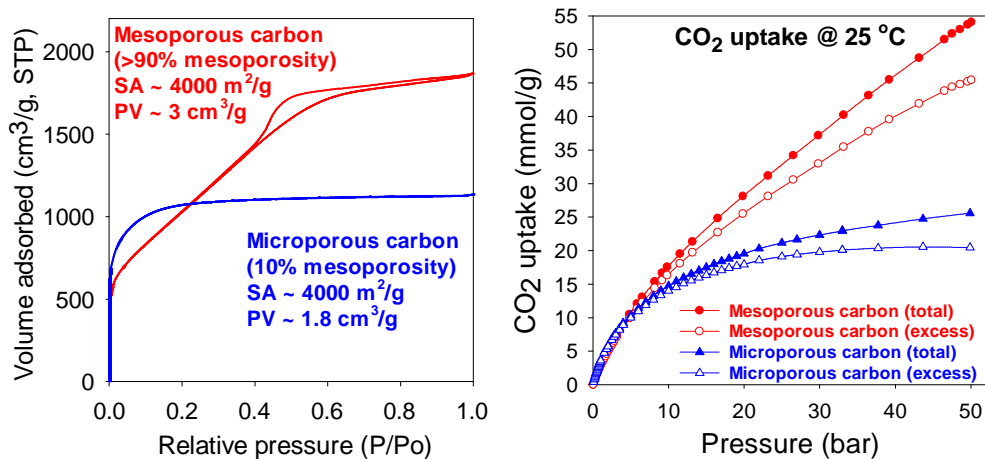
25. E. Haffner-Staton, N. Balahmar and R. Mokaya, *J. Mater. Chem. A* 2016, **4**, 13324.
26. B. Adeniran and R. Mokaya, *J. Mater. Chem. A*, 2015, **3**, 5148.
27. M. Sevilla and A. B. Fuertes, *Energy Environ. Sci.*, 2011, **4**, 1765.
28. G. Srinivas, J. Burrell and T. Yildirim, *Energy Environ. Sci.*, 2012, **5**, 6453.
29. N. P. Wickramaratne and M. Jaroniec, *J. Mater. Chem. A*, 2013, **1**, 112.
30. N. P. Wickramaratne and M. Jaroniec, *ACS Appl. Mater. Interfaces*, 2013, **5**, 1849.
31. Z. Zhang, J. Zhou, W. Xing, Q. Xue, Z. Yan, S. Zhuo and S. Z. Qiao, *Phys. Chem. Chem. Phys.*, 2013, **15**, 2523.
32. B. Adeniran, E. Masika and R. Mokaya, *J. Mater. Chem. A*, 2014, **2**, 14696.
33. X. Fan, L. Zhang, G. Zhang, Z. Shu and J. Shi, *Carbon*, 2013, **61**, 423.
34. H. Wei, S. Deng, B. Hu, Z. Chen, B. Wang, J. Huang and G. Yu, *ChemSusChem*, 2012, **5**, 2354.
35. B. Adeniran and R. Mokaya, *Chem. Mater.* 2016, **28**, 994.
36. H. M. Coromina, D. A. Walsh and R. Mokaya, *J. Mater. Chem. A* 2016, **4**, 280.
37. M. Sevilla, W. Sangchoom, N. Balahmar, A. B. Fuertes and R. Mokaya, *ACS Sust. Chem. Eng.*, 2016, **4**, 4710.
38. J. He, J. W. F. To, P. C. Psarras, H. Yan, T. Atkinson, R. T. Holmes, D. Nordlund, Z. Bao and J. Wilcox, *Adv. Energy Mater.* 2016, **6**, 1502491.
39. A. S. Jalilov, Y. Li, J. Tian, J. M. Tour, *Adv. Energy Mater.* 2017, **7**, 1600693.
40. J. R. Hufton, S. Mayorga and S. Sircar, *AIChE J.* 1999, **45**, 248–256.
41. C. Descamps, C. Bouallou and M. Kanneche, *Energy*, 2008, **33**, 874.
42. A. Agarwal, L. T. Biegler, and S. E. Zitney, *Ind. Eng. Chem. Res.*, 2010, **49**, 5066.
43. S.-I. Yang, D.-Y. Choi, S.-C. Jang, S.-H. Kim and D.-K. Choi, *Adsorption*, 2008, **14**, 583.
44. Z. R. Herm, J. A. Swisher, B. Smit, R. Krishna and J. R. Long, *J. Am. Chem. Soc.*, 2011, **133**, 5664.

45. N. Balahmar, A. M. Lowbridge and R. Mokaya, *J. Mater. Chem. A*, 2016, **4**, 14254.
46. F. Rouquerol, J. Rouquerol and K. Sing, *Adsorption by powders and porous solids: principles, methodology and applications*. 1999, Academic Press: San Diego.
47. M. Sevilla, R. Mokaya and A. B. Fuertes, *Energy Environ. Sci.* 2011, **4**, 2930.
48. M. Sevilla and R. Mokaya, *Energy Environ. Sci.* 2014, **7**, 1250.
49. J.-S. M. Lee, M. E. Briggs, T. Hasell, and A. I. Cooper, *Adv. Mater.* 2016, **28**, 9804.
50. O. K. Farha, A. O. Yazaydin, I. Eryazici, C. D. Malliakas, B. G. Hauser, M. G. Kanatzidis, S. T. Nguyen, R. Q. Snurr and J. T. Hupp, *Nat. Chem.* 2010, **2**, 944.
51. H. Furukawa, N. Ko, Y. B. Go, N. Aratani, S. B. Choi, E. Choi, A. Ö. Yazaydin, R. Q. Snurr, M. O’Keeffe, J. Kim and O. M. Yaghi, *Science* 2010, **329**, 424.
52. H. Furukawa, K. E. Cordova, M. O’Keeffe and O. M. Yaghi, *Science* 2013, **341**, 974.
53. M. E. Casco, M. Martínez-Escandell, J. Silvestre-Albero and F. Rodríguez-Reinoso, *Carbon* 2014, **67**, 230.
54. G. Srinivas, V. Krungleviciute, Z.-X. Guo and T. Yildirim, *Energy Environ. Sci.* 2014, **7**, 335.
55. B. Ashourirad, A. K. Sekizkardes, S. Altarawneh and H. M. El-Kaderi, *Chem. Mater.* 2015, **27**, 1349.
56. Y. Li, T. Ben, B. Zhang, Y. Fu and S. Qiu, *Scientific Reports* 2013, **3**, 2420.
57. J. Purewal, D. Liu, A. Sudik, M. Veenstra, J. Yang, S. Maurer, U. Muller and D. J. Siegel, *J. Phys. Chem. C* 2012, **116**, 20199.
58. J. Purewal, D. Liu, J. Yang, A. Sudik, D. Siegel, S. Maurer and U. Mueller, *Int. J. Hydrogen Energy* 2012, **37**, 2723.
59. A. Dailly and E. Poirier, *Energy Environ. Sci.* 2011, **4**, 3527.
60. R. Zacharia, D. Cossement, L. Lafi and R. Chahine, *J. Mater. Chem.* 2010, **20**, 2145.

61. Y. Peng, V. Krungleviciute, I. Eryazici, J. T. Hupp, O. K. Farha and T. Yildirim, *J. Am. Chem. Soc.* 2013, **135**, 11887
62. A. L. Myers and J. M. Prausnitz, *AIChE J.*, 1965, **11**, 121.

Graphical Abstract

Mesoporous carbons (with up to 95% of pore volume from mesopores) with surface area and pore volume of $\sim 4000 \text{ m}^2\text{g}^{-1}$ and $\sim 3.6 \text{ cm}^3\text{g}^{-1}$, respectively, are excellent CO_2 absorbers under pre combustion conditions and can store 55 mmol g^{-1} (i.e., 2.42 g g^{-1}) or 930 g l^{-1} at $25 \text{ }^\circ\text{C}$ and 50 bar .



Supporting Information

**Ultra-high surface area mesoporous carbons for colossal pre combustion
CO₂ capture and storage as materials for hydrogen purification**

Michael Cox, and Robert Mokaya

School of Chemistry, University of Nottingham, University Park, NG7 2RD Nottingham, UK.

*r.mokaya@nottingham.ac.uk

Table S1. Textural properties of polypyrrole-derived activated (PPY-xT) and compactivated (MPPY-4800) carbons compared to other carbons and porous materials that possess varying levels of mesoporosity.

Sample	Surface area (m ² g ⁻¹)	Pore volume ^a (cm ³ g ⁻¹)	Mesoporosity ^b (%)	Reference
CA-4700	3771	1.75 (0.21)	12	This work
AC-0	3100	1.46 (0.41)	28	1
SU-AC-400	4196	2.26 (0.70)	31	2
AC-2M	3420	2.22 (0.94)	42	1
UGil-900	4200	2.41 (n.d.)		3
PPY-4700	3568	2.46 (2.18)	89	This work
PPY-4800	3589	2.71 (2.46)	91	This work
MPPY-4800	3934	2.92 (2.72)	93	This work
PPY-5800	2974	2.85 (2.63)	92	This work
PPY-3900	3285	2.60 (2.30)	88	This work
PPY-4900	2842	2.77 (2.50)	90	This work
PPY-5900	2798	3.54 (3.35)	95	This work
MOF-210	6240	3.60 (n.d.)		4
NU-100	6143	2.82 (n.d.)		5

^aThe values in the parenthesis refer to mesopore volume. ^bProportion of pore volume arising from mesopores. (n.d. = not determined)

References

1. M. Sevilla, W. Sangchoom, N. Balahmar, A. B. Fuertes and R. Mokaya, *ACS Sust. Chem. Eng.*, 2016, **4**, 4710.
2. J. He, J. W. F. To, P. C. Psarras, H. Yan, T. Atkinson, R. T. Holmes, D. Nordlund, Z. Bao and J. Wilcox, *Adv. Energy Mater.* 2016, **6**, 1502491.
3. A. S. Jalilov, Y. Li, J. Tian, J. M. Tour, *Adv. Energy Mater.* 2017, **7**, 1600693.
4. H. Furukawa, N. Ko, Y. B. Go, N. Aratani, S. B. Choi, E. Choi, A. Ö. Yazaydin, R. Q. Snurr, M. O’Keeffe, J. Kim and O. M. Yaghi, *Science* 2010, **329**, 424.
5. O. K. Farha, A. O. Yazaydin, I. Eryazici, C. D. Malliakas, B. G. Hauser, M. G. Kanatzidis, S. T. Nguyen, R. Q. Snurr and J. T. Hupp, *Nat. Chem.* 2010, **2**, 944.

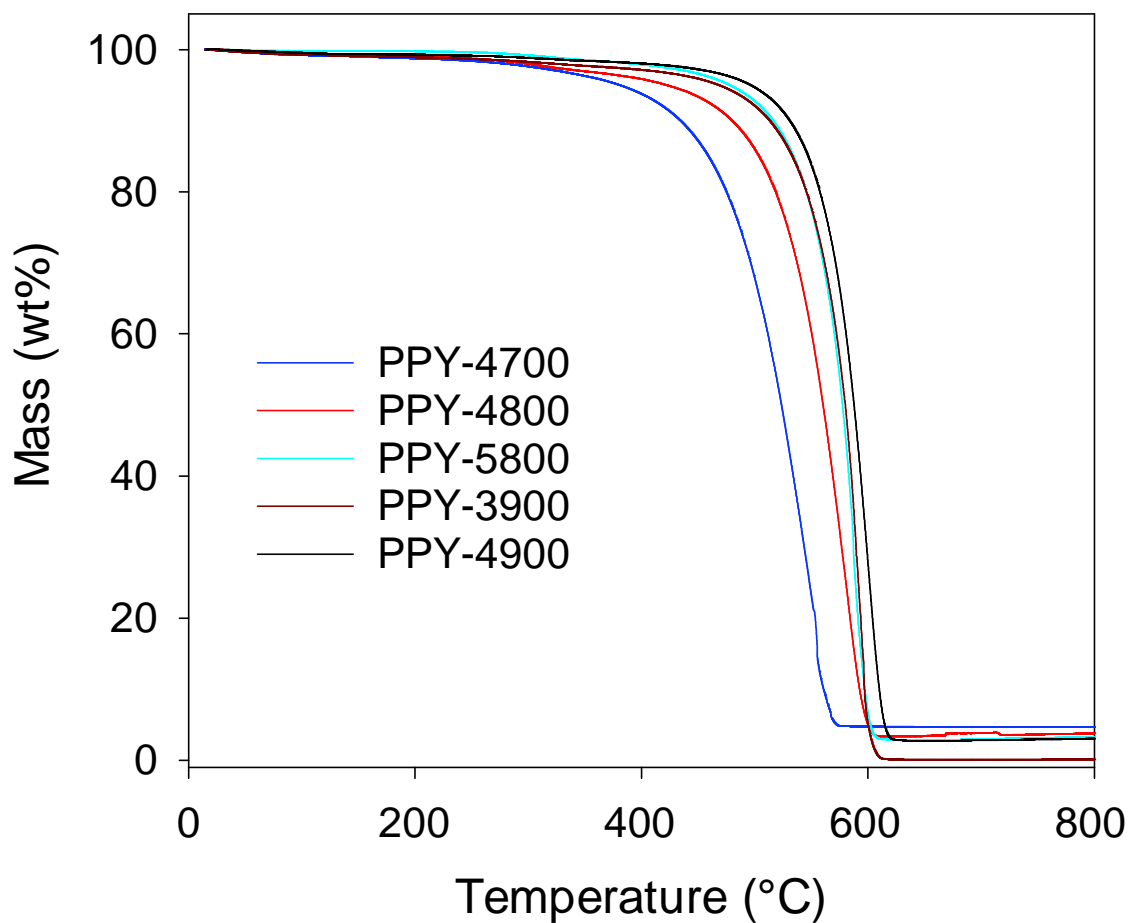
Table S2. Total and excess gravimetric CO₂ uptake of polypyrrole-derived activated (PPY-xT) carbons and compactivated (MPPY-4800) carbon compared to other carbons and metal organic frameworks (MOFs).

Sample	CO ₂ uptake ^a (mmol g ⁻¹)					Reference
	1 bar	20 bar	30 bar	40 bar	50 bar	
CA-4700	3.7	19.5 (18.0)	22.3 (19.8)	24.1 (20.4)	25.6 (20.5)	This work
AC-0	2.4	20.4 (19.2)	24.6 (22.5)	27.1 (24.1)	28.5 (24.2)	1
AC-2M	2.3	22.8 (20.7)	29.2 (26.0)	34.5 (29.7)	38.3 (31.7)	1
SU-AC-400	4.3	22.4 (20.3)	28.3 (25.1)	32.5 (27.5)	34.9 (28.3)	2
UGil-900	2.6	22.9 (21.5)	29.4 (27.0)	33.9 (29.6)	35.2 (30.8)	3
PPY-4700	2.3	22.8 (20.6)	29.6 (26.0)	35.4 (30.2)	40.3 (32.9)	This work
PPY-4800	2.5	25.0 (22.5)	33.0 (29.0)	39.5 (34.0)	45.3 (37.2)	This work
MPPY-4800	2.8	28.1 (25.5)	37.2 (33.0)	45.6 (39.5)	54.1 (45.4)	This work
PPY-5800	1.3	24.1 (21.5)	32.8 (28.7)	41.8 (35.8)	50.8 (42.3)	This work
PPY-3900	2.2	23.2 (20.9)	30.7 (26.9)	37.5 (32.0)	44.5 (36.5)	This work
PPY-4900	2.0	23.6 (21.2)	31.9 (27.9)	41.4 (34.4)	49.3 (41.0)	This work
PPY-5900	2.1	25.7 (22.5)	34.9 (29.7)	44.6 (37.1)	55.1 (44.5)	This work
MOF-210	0.9	19.2 (16.0)	38.9 (33.7)	55.0 (46.7)	64.2 (52.5)	4
NU-100	2.7	24.6 (22.0)	40.9 (36.3)	52.7 (46.8)		5

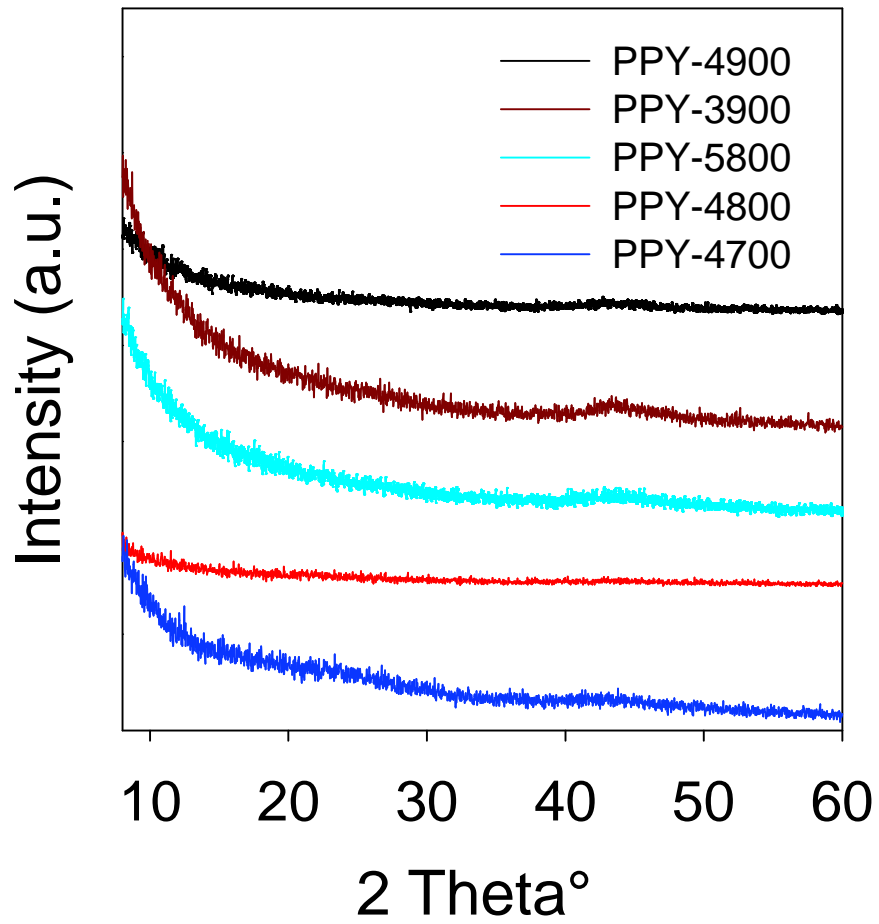
^aCO₂ uptake at 25 °C and various pressures (i.e., 1, 20, 30, 40 and 50 bar). The values in the parenthesis are excess CO₂ uptake.

References

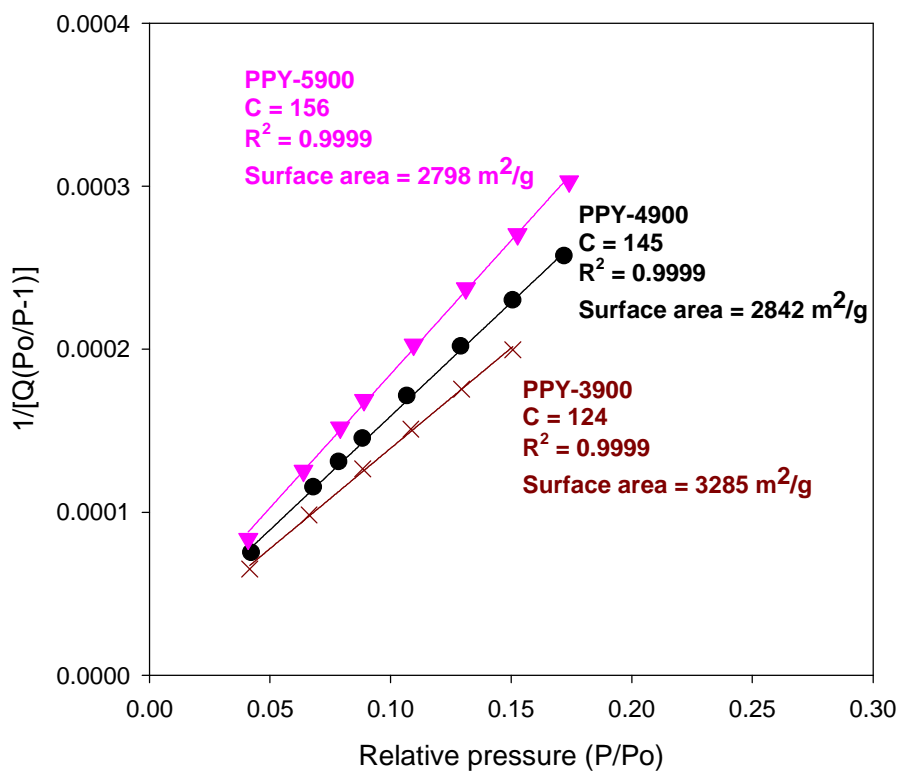
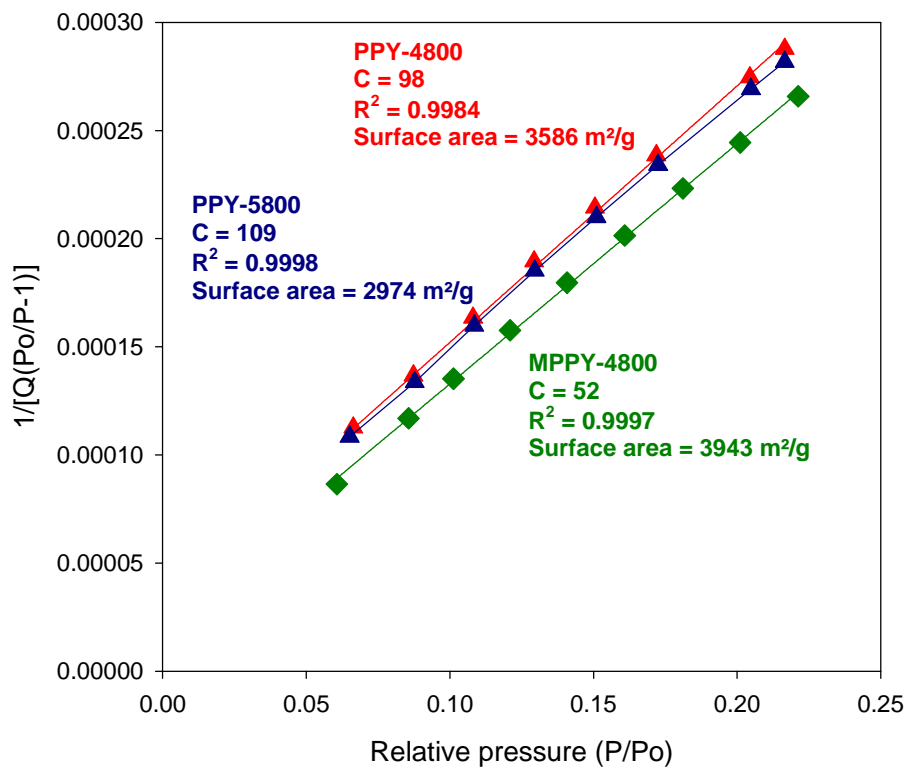
- M. Sevilla, W. Sangchoom, N. Balahmar, A. B. Fuertes and R. Mokaya, *ACS Sust. Chem. Eng.*, 2016, **4**, 4710.
- J. He, J. W. F. To, P. C. Psarras, H. Yan, T. Atkinson, R. T. Holmes, D. Nordlund, Z. Bao and J. Wilcox, *Adv. Energy Mater.* 2016, **6**, 1502491.
- A. S. Jalilov, Y. Li, J. Tian, J. M. Tour, *Adv. Energy Mater.* 2017, **7**, 1600693.
- H. Furukawa, N. Ko, Y. B. Go, N. Aratani, S. B. Choi, E. Choi, A. Ö. Yazaydin, R. Q. Snurr, M. O’Keeffe, J. Kim and O. M. Yaghi, *Science* 2010, **329**, 424.
- O. K. Farha, A. O. Yazaydin, I. Eryazici, C. D. Malliakas, B. G. Hauser, M. G. Kanatzidis, S. T. Nguyen, R. Q. Snurr and J. T. Hupp, *Nat. Chem.* 2010, **2**, 944.



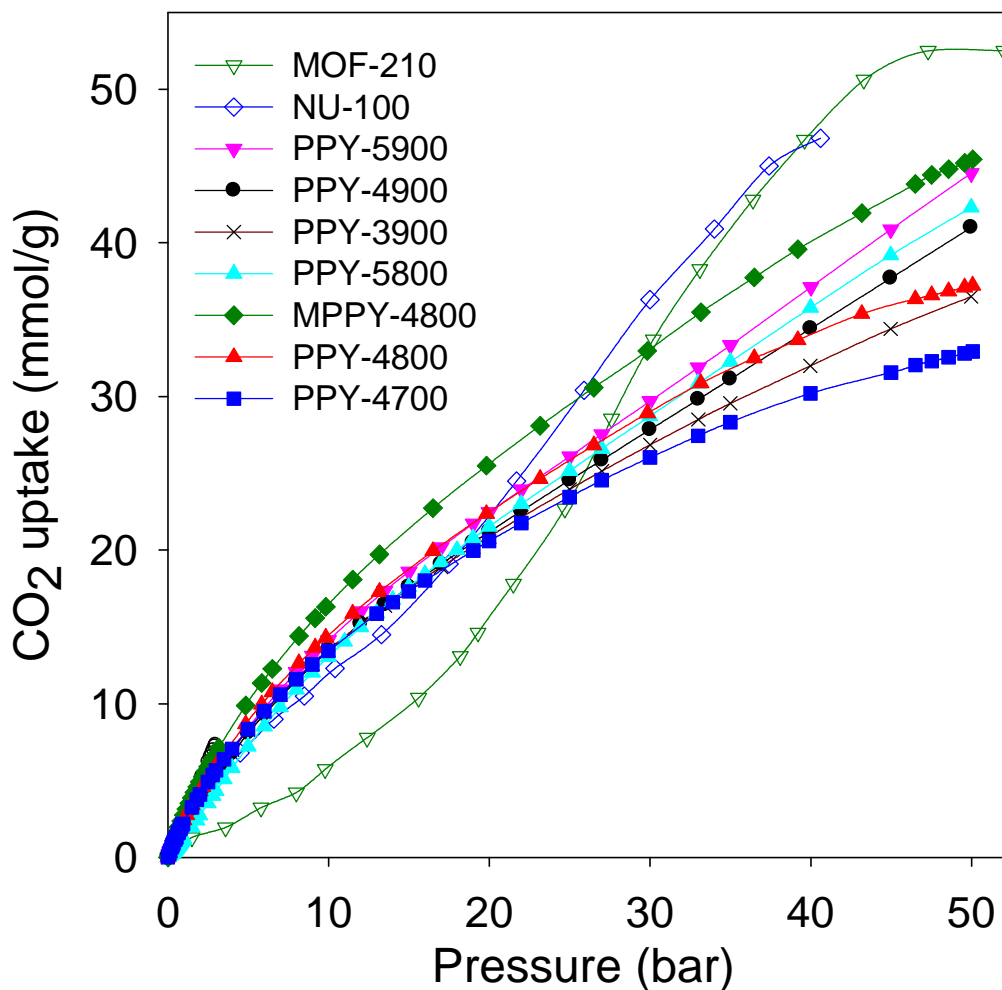
Supporting Figure S1. Thermogravimetric analysis (TGA) curves of polypyrrole-derived activated (PPY-xT) carbons heated in air.



Supporting Figure S2. Powder XRD patterns of polypyrrole-derived activated (PPY-xT) carbons.



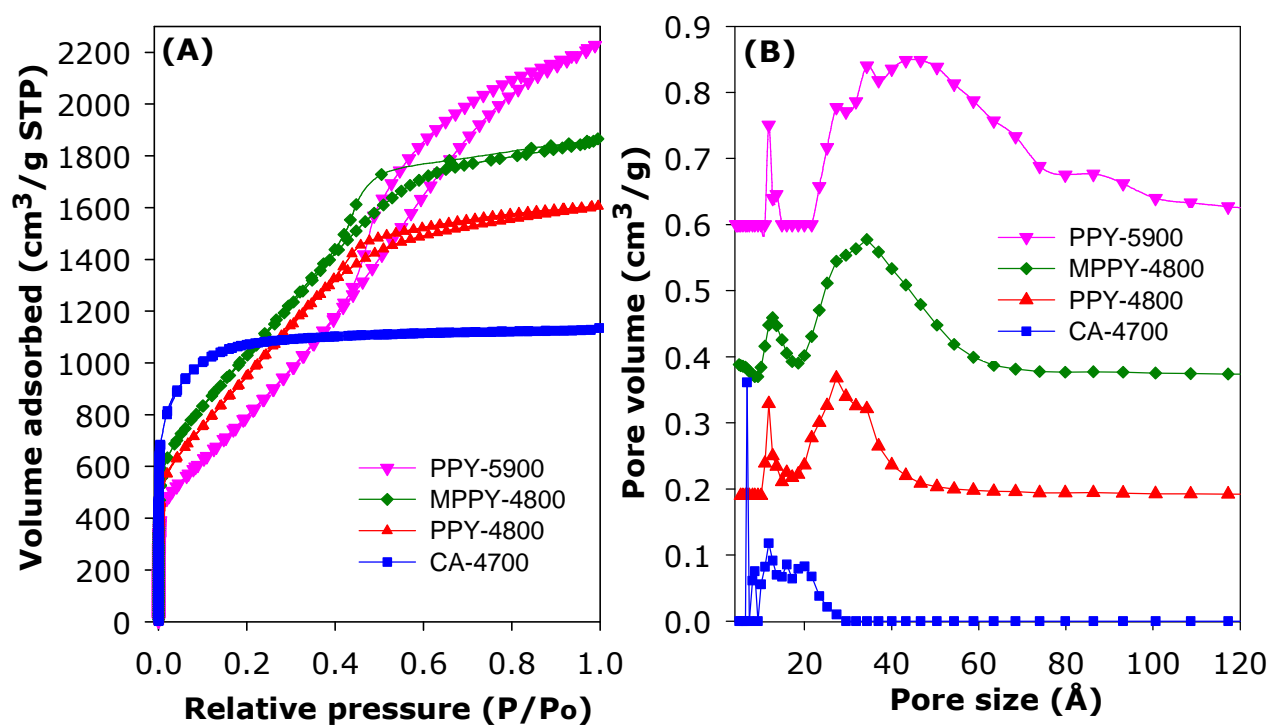
Supporting Figure S3. Rouquerel plots used to calculate the BET surface area of polypyrrole-derived activated (PPY-xT) carbons. We also show the values of the BET (or C) constants.



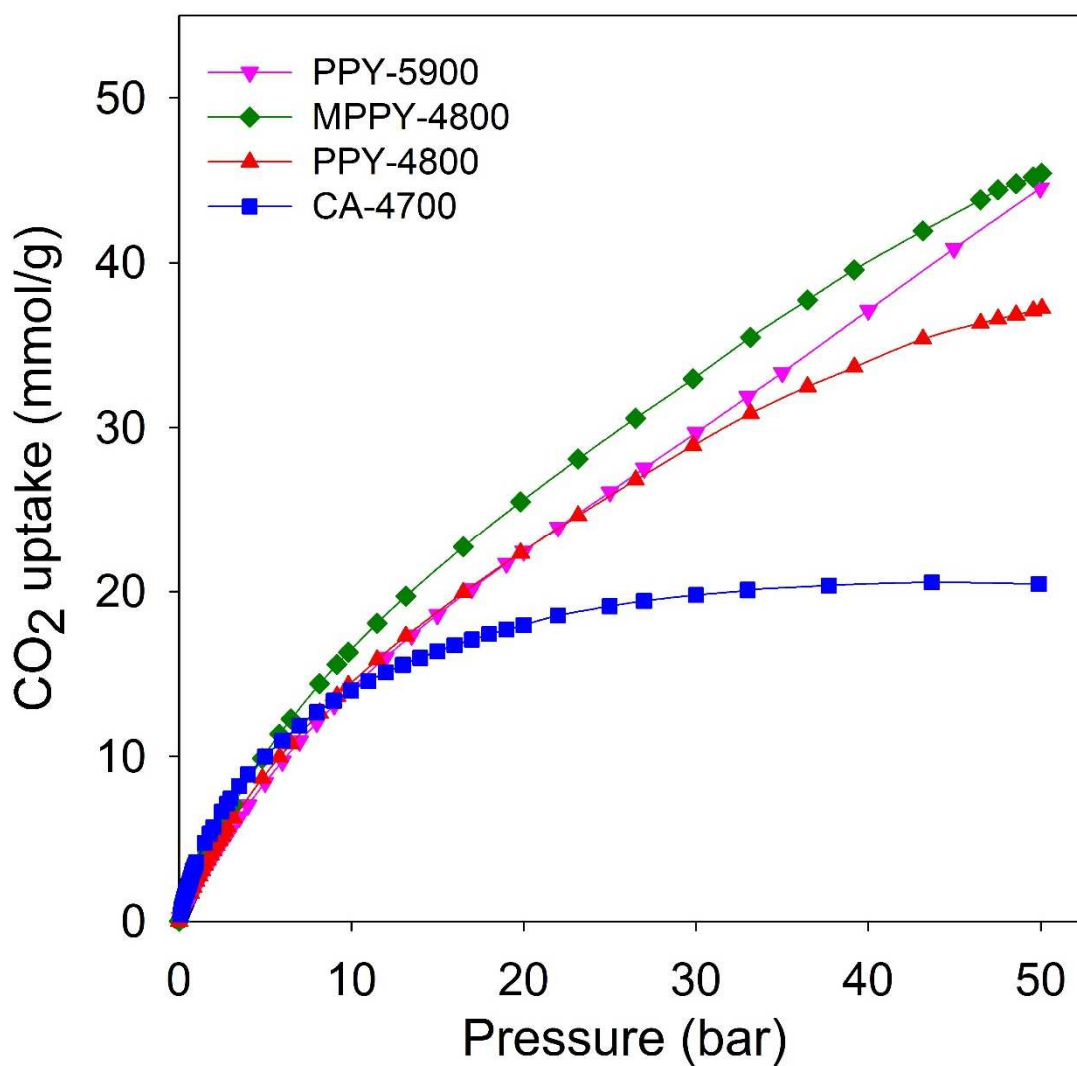
Supporting Figure S4. Excess CO₂ uptake of polypyrrole-derived activated (PPY-xT) carbons, compactivated (MPPY-4800) carbon and benchmark MOFs (MOF-210 and NU-100)* at 25 °C and pressure of 0 – 50 bar.

*Data for MOF-210 is taken from reference 51 (O. K. Farha, A. O. Yazaydin, I. Eryazici, C. D. Malliakas, B. G. Hauser, M. G. Kanatzidis, S. T. Nguyen, R. Q. Snurr and J. T. Hupp, *Nat. Chem.* 2010, **2**, 944).

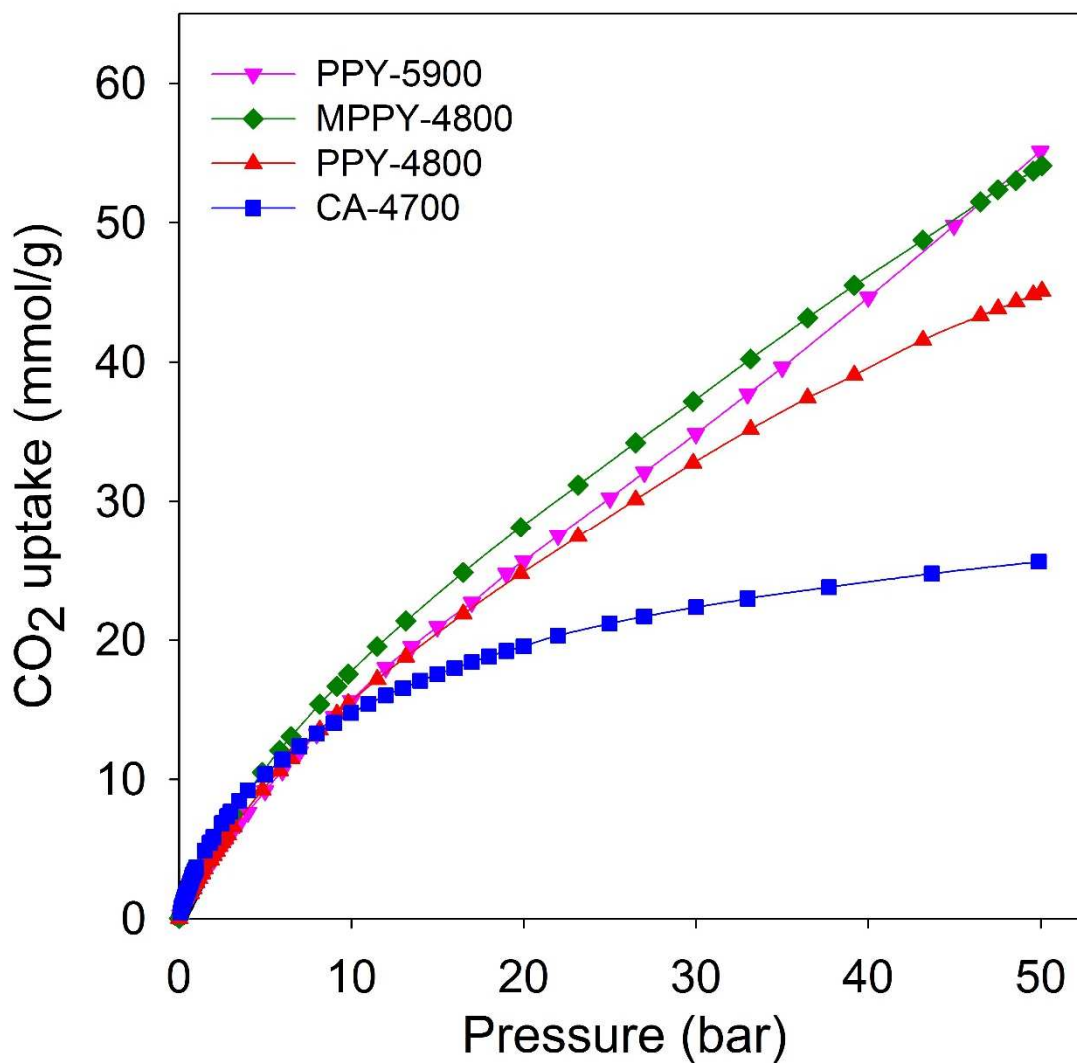
*Data for NU-100 is taken from reference 50 (H. Furukawa, N. Ko, Y. B. Go, N. Aratani, S. B. Choi, E. Choi, A. Ö. Yazaydin, R. Q. Snurr, M. O’Keeffe, J. Kim and O. M. Yaghi, *Science* 2010, **329**, 424).



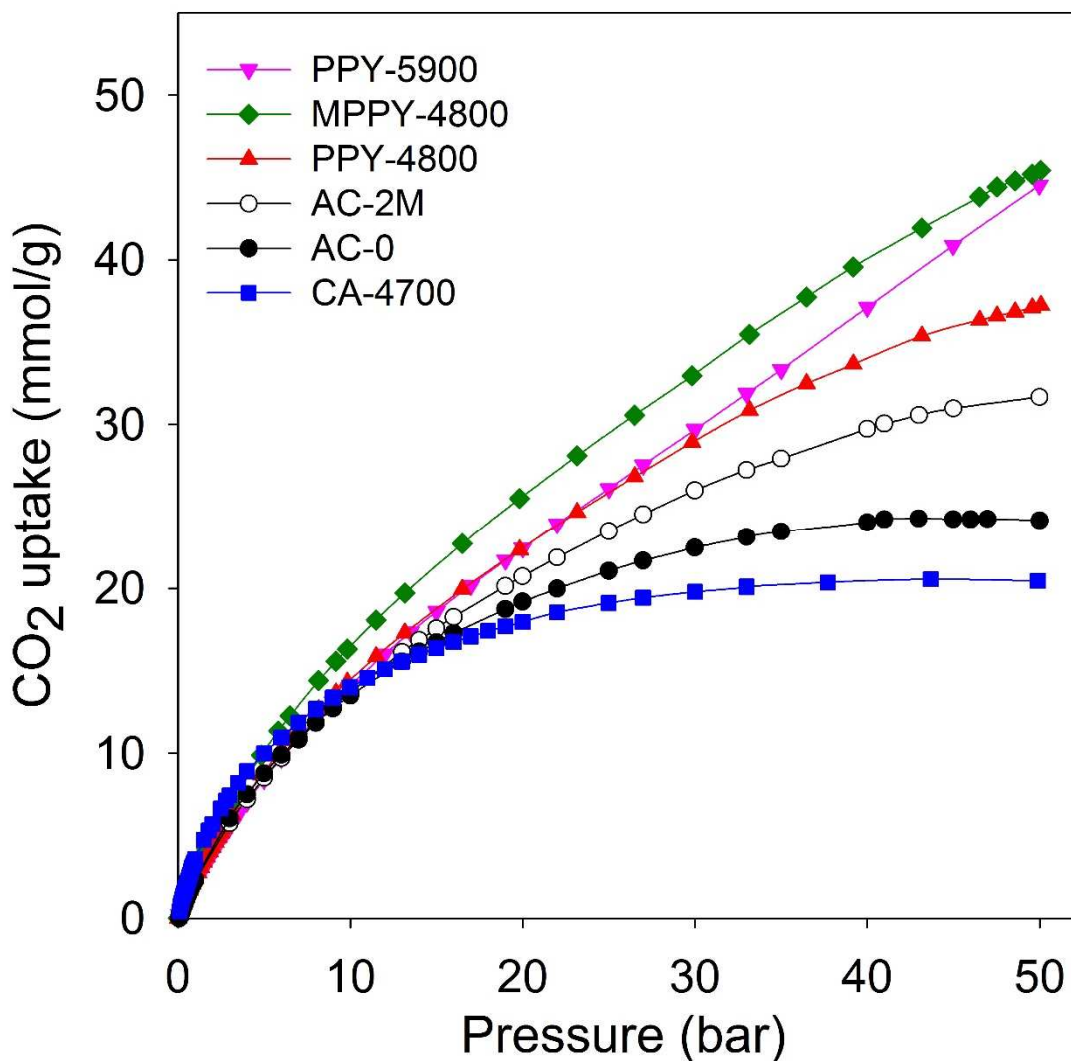
Supporting Figure S5. Nitrogen sorption isotherms (A) and corresponding pore size distribution (PSD) curves (B) of mesoporous polypyrrole-derived (PPY-xT) activated carbons, a compactivated (MPPY-4800) carbon, and a microporous activated carbon (CA-4700).



Supporting Figure S6. Excess CO₂ uptake of polypyrrole-derived activated (PPY-xT) carbons, compactivated (MPPY-4800) carbon, and a microporous activated carbon (CA-4700).

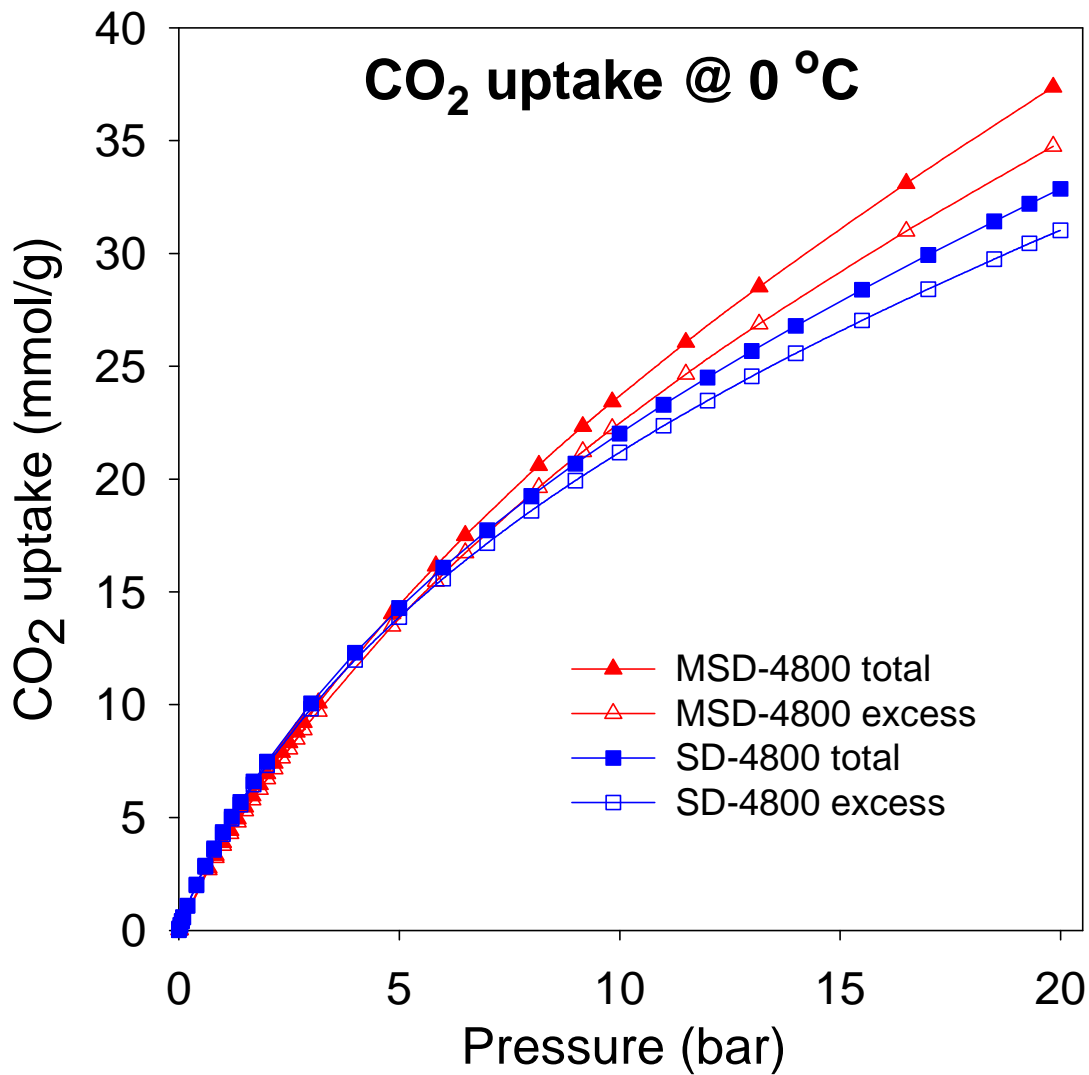


Supporting Figure S7. Total CO₂ uptake of polypyrrole-derived activated (PPY-xT) carbons, compactivated (MPPY-4800) carbon, and a microporous activated carbon (CA-4700).

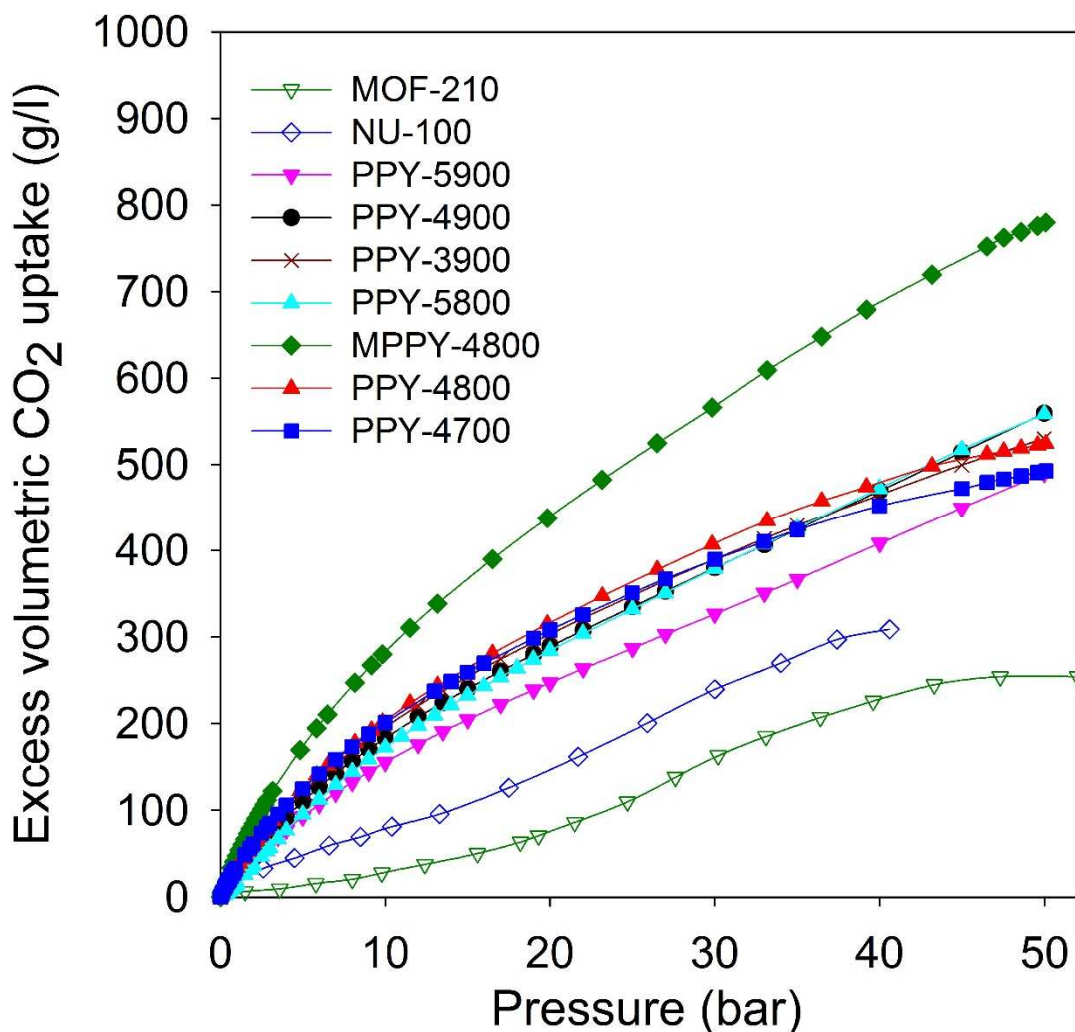


Supporting Figure S8. Excess CO₂ uptake of polypyrrole-derived activated (PPY-xT) carbons, compactivated (MPPY-4800) carbon, a microporous activated carbon (CA-4700) and micro/mesoporous activated carbons (AC-0 and AC-2M)*.

*Data for AC-0 and AC-2M is taken from reference 37 (M. Sevilla, W. Sangchoom, N. Balahmar, A. B. Fuertes and R. Mokaya, *ACS Sust. Chem. Eng.*, 2016, **4**, 4710).



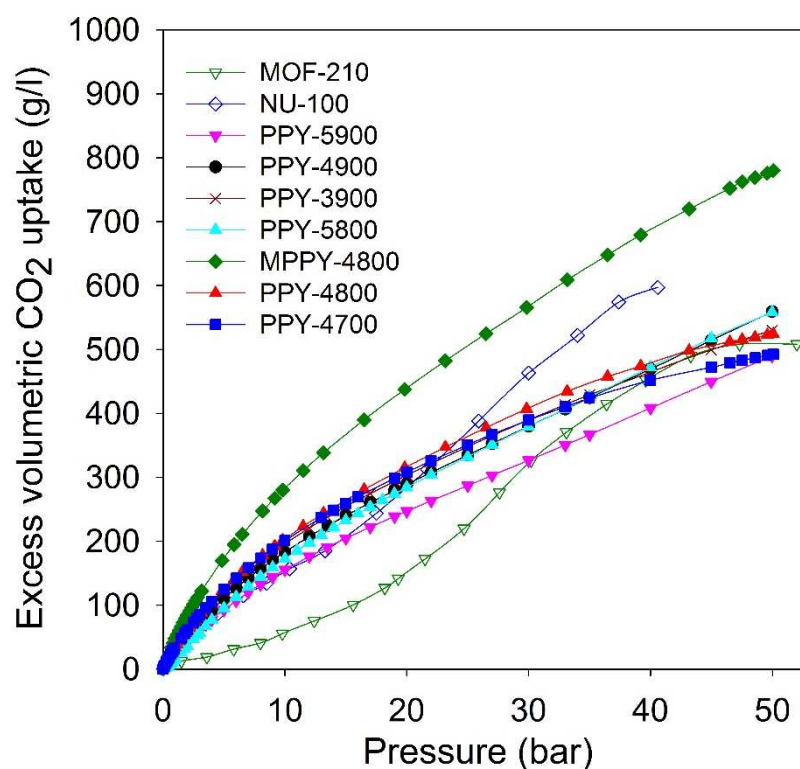
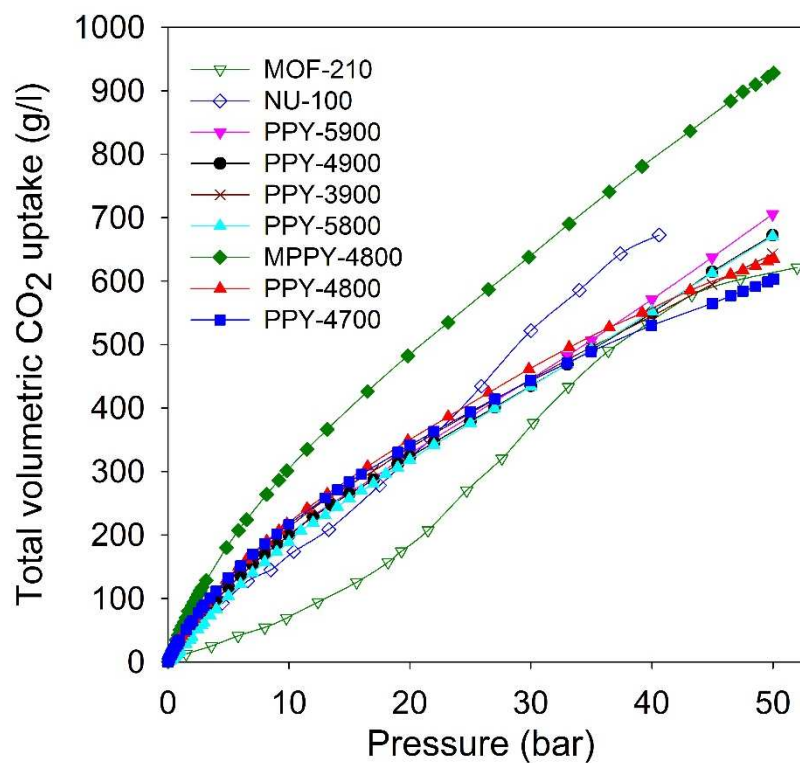
Supporting Figure S9. Total and excess CO₂ uptake at 0 °C for activated (SD-4800) and compactivated (MSD-4800) carbon derived from wood sawdust.



Supporting Figure S10. Excess volumetric CO₂ uptake of polypyrrole-derived activated (PPY-xT) carbons, compactivated (MPPY-4800) carbon and benchmark MOFs (MOF-210 and NU-100) at 25 °C and pressure of 0 – 50 bar. Packing density values (g cm⁻³) used are: 0.15 (NU-100) and 0.12 (MOF-210) according to reference 61 (Y. Peng, V. Krungleviciute, I. Eryazici, J. T. Hupp, O. K. Farha and T. Yildirim, *J. Am. Chem. Soc.* 2013, **135**, 11887–11894).

*CO₂ uptake data for MOF-210 is taken from reference 51 (O. K. Farha, A. O. Yazaydin, I. Eryazici, C. D. Malliakas, B. G. Hauser, M. G. Kanatzidis, S. T. Nguyen, R. Q. Snurr and J. T. Hupp, *Nat. Chem.* 2010, **2**, 944).

*CO₂ uptake data for NU-100 is taken from reference 50 (H. Furukawa, N. Ko, Y. B. Go, N. Aratani, S. B. Choi, E. Choi, A. Ö. Yazaydin, R. Q. Snurr, M. O’Keeffe, J. Kim and O. M. Yaghi, *Science* 2010, **329**, 424).



Supporting Figure S11. Total (top) and excess (bottom) CO₂ uptake of activated (PPY-xT) carbons, compactivated (MPPY-4800) carbon and MOFs (MOF-210 and NU-100) at 25 °C. Crystal density of 0.25 and 0.30 g cm⁻³, respectively, was used to estimate the volumetric uptake of MOF-210 and NU-100. CO₂ uptake data for the MOFs is adapted from reference 50 and 51.